

# **Study of Spatial and Transform Domain Filters for Efficient Noise Reduction**

A Thesis Submitted to  
National Institute Of Technology, Rourkela  
IN PARTIAL FULFILMENT OF THE REQUIRMENTS FOR THE  
DEGREE OF

**MASTER OF TECHNOLOGY**

In  
**TELEMATICS AND SIGNAL PROCESSING**

By  
**ANIL KUMAR KANITHI**  
**Roll No: 209EC1105**



DEPARTMENT OF ELECTRONICS AND COMMUNICATION  
ENGINEERING  
NATIONAL INSTITUTE OF TECHNOLOGY  
ROURKELA, INDIA

2011

# **Study of Spatial and Transform Domain Filters for Efficient Noise Reduction**

A Thesis Submitted to  
National Institute Of Technology, Rourkela

IN PARTIAL FULFILMENT OF THE REQUIRMENTS FOR THE  
DEGREE OF

**MASTER OF TECHNOLOGY**  
In  
**TELEMATICS AND SIGNAL PROCESSING**

By  
**ANIL KUMAR KANITHI**  
Roll No: 209EC1105

Under The Guidance of  
**Dr. Sukadev Meher**



DEPARTMENT OF ELECTRONICS AND COMMUNICATION  
ENGINEERING  
NATIONAL INSTITUTE OF TECHNOLOGY  
ROURKELA, INDIA

2011



NATIONAL INSTITUTE OF TECHNOLOGY  
ROURKELA

CERTIFICATE

This is to certify that the thesis entitled, “**Study of Spatial and Transform Domain Filters For Efficient Noise Reduction**” submitted by **ANIL KUMAR KANITHI** in partial fulfillment of the requirements for the award of Master of Technology Degree in **Electronics & Communication Engineering** with specialization in **Telematics and Signal Processing** during 2010-2011 at the National Institute of Technology, Rourkela, is an authentic work carried out by him under my supervision and guidance.

**Dr. Sukadev Meher**

Dept. of Electronics & Communication Engg

National Institute of Technology

Rourkela-769008

## ACKNOWLEDGEMENTS

I express my indebtedness and gratefulness to my teacher and supervisor. **Dr.Sukadev Meher** for his continuous encouragement and guidance. His advices have value lasting much beyond this project. I am indebted to him for the valuable time he has spared for me during this work.

I am thankful to Prof. S.K. Patra, Head of the Department of Electronics & Communication Engineering who provided all the official facilities to me.

I would like to express my humble respects to Prof. G. S. Rath, Prof. K. K. Mahapatra, Prof. S. K. Behera, Prof. D.P.Acharya, Prof.A.K.Sahoo and N.V.L.N.Murthy for teaching me and also helping me how to learn. And also I would like to thanks all faculty members of ECE. Department for their help and guidance. They have been great sources of inspiration to me and I thank them from the bottom of my heart.

I would to like express my thanks to my seniors colleagues of digital image processing lab and friends for their help during the research period. I've enjoyed their companionship so much during my stay at NIT, Rourkela.

Last but not least I would like to thank my parents, who taught me the value of hard work by their own example. They rendered me enormous support being apart during the whole tenure of my stay in NIT Rourkela.

ANIL KUMAR KANITHI

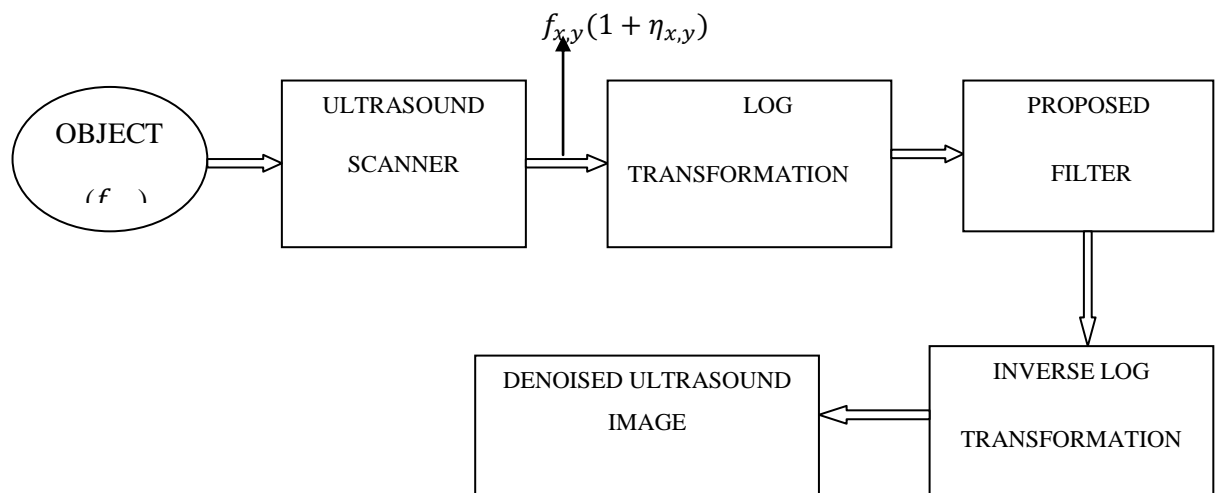
ROLL NO. 209EC1105

Dept. of E&CE, NIT, ROURKELA

## ABSTRACT

Image Denoising is an important pre-processing task before further processing of image like segmentation, feature extraction, texture analysis etc. The purpose of denoising is to remove the noise while retaining the edges and other detailed features as much as possible. This noise gets introduced during acquisition, transmission & reception and storage & retrieval processes. As a result, there is degradation in visual quality of an image. The noises considered in this thesis Additive Gaussian White Noise (AWGN), Impulsive Noise and Multiplicative (Speckle) Noise. Among the currently available medical imaging modalities, ultrasound imaging is considered to be noninvasive, practically harmless to the human body, portable, accurate, and cost effective. Unfortunately, the quality of medical ultrasound is generally limited due to Speckle noise, which is an inherent property of medical ultrasound imaging, and it generally tends to reduce the image resolution and contrast, thereby reducing the diagnostic value of this imaging modality. As a result, speckle noise reduction is an important prerequisite, whenever ultrasound imaging is used for tissue characterization.

Among the many methods that have been proposed to perform this task, there exists a class of approaches that use a multiplicative model of speckled image formation and take advantage of the logarithmical transformation in order to convert multiplicative speckle noise into additive noise. The common assumption made in a dominant number of such studies is that the samples of the additive noise are mutually uncorrelated and obey a Gaussian distribution. Now the noise became AWGN.



Many spatial-Domain filters such as Mean filter, Median filter, Alpha-trimmed mean filter, Wiener filter, Anisotropic diffusion filter, Total variation filter, Lee filter, Non-local means filter, Bilateral filter etc. are in literature for suppression of AWGN. Also many Wavelet-domain filters such as VisuShrink, SureShrink, BayesShrink, Locally adaptive window maximum likelihood estimation etc. are proposed to suppress the AWGN effectively. The recently developed Circular Spatial Filter (CSF) also performed efficiently under high variance of noise. Performance of these filters are compared with the existing filters in terms of peak-signal-to-noise-ratio (PSNR), universal quality index (UQI) and execution time (ET). The Mean filter Gaussian noise under low noise conditions efficiently. On the other hand CSF performs well under moderate and high noise conditions. It is also capable of retaining the edges and intricate details of the image. In this filter, filtering window is combination of distance kernel and gray level kernel. we can also make adaptive the window size of CSF depends on noise variance. where the size of the window varies with the level of complexity of a particular region in an image and the noise power as well. A smooth or flat region (also called as homogenous region) is said to be less complex as compared to an edge region. The region containing edges and textures are treated as highly complex regions. The window size is increased for a smoother region and also for an image with high noise power.

. From the wavelets properties and behavior, they play a major role in image compression and image denoising. Wavelet coefficients calculated by a wavelet transform represent change in the time series at a particular resolution. By considering the time series at various resolutions, it is then possible to filter out the noise. The wavelet equation produces different types of wavelet families like Daubechies, Haar, symlets, coiflets, etc. .Wavelet Thresholding is the another important area in wavelet domain filtering. Wavelet filters, Visu Shrink, Sure Shrink, Bayes Shrink, Neigh Shrink, Oracle Shrink, Smooth Shrink are the some of filtering techniques to remove the noise from noisy images. We can apply fuzzy techniques to wavelet domain filters to the complexity.

## Contents

1.Introduction.....	i
Preview .....	1
1.1 Fundamentals of Digital Image Processing .....	1
1.2 The Problem Statement.....	4
1.3 Thesis Layout.....	4
2. Noise in Digital Image .....	1
2.1 Noise in Digital Images .....	5
2.1.1 Gaussian Noise.....	5
2.1.2 Salt and Pepper Noise .....	7
2.1.3 Speckle Noise.....	8
2.2 Image Metrics .....	9
2.2.1 Mean Square Error.....	10
2.2.2 Peak signal to noise ratio (PSNR).....	10
2.2.3 Universal Quality Index .....	10
2.2.4 Execution Time .....	11
2.3 Literature Review.....	12
2.3.1 Bilateral Filter .....	13
2.3.2 Circular Spatial Filter(CSF).....	14
2.3.3 Adaptive Circular Spatial Filter .....	17
2.4 Simulation Results .....	18
3.Linear and Nonlinear Filtering.....	5
3.1 Background.....	20
3.2 Spatial Filters .....	21
3.2.1 Mean Filter.....	21
3.2.2 Median Filter.....	23
3.2.3 Wiener Filter .....	24
3.2.4 Lee Filter.....	25
3.2.5 Anisotropic Diffusion (AD) Filter .....	26

3.2.6 Total Variation (TV) Filter .....	28
3.3 Simulation Results .....	29
4.Wavelet Domain Filtering.....	20
4.1 Discrete Wavelet Transform (DWT) .....	36
4.2 Properties of DWT .....	37
4.3 Wavelet Thresholding .....	38
4.4 Types of Wavelet Denoising .....	42
4.4.1 VisuShrink .....	42
4.4.2 SureShrink.....	43
4.4.3 BayesShrink .....	43
4.4.4 OracleShrink and OracleThresh.....	44
4.4.5 NeighShrink .....	45
4.4.6 Smooth Shrink .....	45
4.5 Fuzzy based Wavelet Shinkage.....	47
4.5.1 Introduction of fuzzy Logic .....	47
4.5.2 Procedure for fuzzy based wavelet shrinkage denoising .....	48
technique[4] .....	48
4.6 Simulation Results .....	51
5.Conclusion and Future Work .....	63
5.1 Conclusion .....	61
5.2 Scope for future Work .....	62
References.....	63

## List of Figures

Figure 2.1	Gaussian Noise Distribution	8
Figure 2.2	Gaussian noise(mean 0, variance 0.05)	8
Figure 2.3	Probability Density Function of SPN gray level	9
Figure 2.4	salt and pepper noise variance of 0.05	9
Figure 2.5	Gamma Distribution	10
Figure 2.6	Speckle Noise with variance 0.05	10
Figure 2.7	circular window for CSF	19
Figure 4.1	Hard Thresholding	42
Figure 4.2	Soft Thresholding	43
Figure 4.3	Two level wavelet decomposition of lenna image	45
Figure 4.4	Triangular membership function	50
Figure 4.6	membership function for large coefficient	54
Figure 4.7	membership function for large variable	54

## List of Tables

Table 2.1	Performance of Spatial Filters in terms of PSNR	21
Table 3.1	3X3 mask of Mean Filter	25
Table 3.2	Neighbourhood of particular pixel	26
Table 3.3	Constant weight filter	26
Table 3.4	Median values in the neighbourhood of 140	27
Table 3.5	Filtering Performance of Spatial Domain filters in terms of PSNR (dB) operated on Goldhill image	34
Table 3.6	Filtering Performance of Spatial Domain filters in terms of UQI operated on Goldhill image	35
Table 4.1	Wavelet families and their properties	40
Table 4.2	2-D Wavelet Decomposition	44
Table 4.3	3X3 directional window	49
Table 4.4	Filtering Performance of Wavelet Domain filters in terms of PSNR (dB) operated on MRI image of Brain under AWGN.	54
Table 4.5	Filtering Performance of Wavelet Domain filters in terms of UQI operated on MRI image of Brain under AWGN.	54
Table 4.6	Filtering Performance of Wavelet Domain filters in terms of PSNR (dB) operated on MRI image of Brain under Speckle Noise	55
Table 4.7	Filtering Performance of Wavelet Domain filters in terms of UQI operated on MRI image of Brain under Speckle noise	55
Table 4.8	Filtering Performance of Wavelet Domain filters in terms of PSNR (dB) operated on ultrasound image of baby	56
Table 4.9	Filtering Performance of Wavelet Domain filters in terms of UQI operated on ultrasound image of baby(Speckle Noise)	
Table 4.10	Execution time of wavelet domain filters	57

# Chapter 1

## **Introduction**

## Preview

Vision is a complicated process that requires numerous components of the human eye and brain to work together. The sense of vision has been one of the most vital senses for human survival and evolution. Humans use the visual system to see or acquire visual information, perceive, i.e. process and understand it and then deduce inferences from the perceived information. The field of image processing focuses on automating the process of gathering and processing visual information. The process of receiving and analyzing visual information by digital computer is called *digital image processing*. It usually refers to the processing of a 2-dimensional (2-D) picture signal by a digital hardware. The 2-D image signal might be a photographic image, text image, graphic image (including synthetic image), biomedical image (X-ray, ultrasound, etc.), satellite image, etc. Fundamentals of Digital Image Processing are discussed in this chapter, which follows various metrics used to analyze the filters used.

## 1.1 Fundamentals of Digital Image Processing

An image may be described as a two-dimensional function  $I$ .

$$I = f(x, y)$$

where  $x$  and  $y$  are spatial coordinates. Amplitude of  $f$  at any pair of coordinates  $(x, y)$  is called intensity  $I$  or gray value of the image. When spatial coordinates and amplitude values are all finite, discrete quantities, the image is called digital image.

Digital image processing may be classified into various sub branches based on methods whose:

- inputs and outputs are images and
- inputs may be images where as outputs are attributes extracted from those images.

Following is the list of different image processing functions based on the above two classes.

- (i) Image Acquisition
- (ii) Image Enhancement
- (iii) Image Restoration
- (iv) Color Image Processing

- (v) Transform-domain Processing
- (vi) Image Compression
- (vii) Morphological Image Processing
- (viii) Image segmentation
- (ix) Image Representation and Description
- (x) Object Recognition

For the first seven image processing functions the inputs and outputs are images where as for the last three the outputs are attributes from the input images. Above all functions, With the exception of image acquisition and display are implemented in software.

Image processing may be performed in the spatial-domain or in a transform-domain. Depending on the application, a efficient transform, e.g. discrete Fourier transform (DFT) , discrete cosine transform (DCT) , discrete Hartley transform (DHT) , discrete wavelet transform (DWT) , etc., may be employed.

Image enhancement is subjective area of image processing. These techniques are used to highlight certain features of interest in an image. Two important examples of image enhancement are: (i) increasing the contrast, and (ii) changing the brightness level of an image so that the image looks better.

Image restoration is one of the prime areas of image processing and it is very much objective .The restoration techniques are based on mathematical and statistical models of image degradation. Denoising and Deblurring tasks come under this category.Its objective is to recover the images from degraded observations. The techniques involved in image restoration are oriented towards modeling the degradations and then applying an inverse procedure to obtain an approximation of the original image. Hence, it may be treated as a deconvolution operation.

Depending on applications, there are various types of imaging systems. X-ray, Gamma ray, ultraviolet, and ultrasonic imaging systems are used in biomedical instrumentation. In astronomy, the ultraviolet, infrared and radio imaging systems are used. Sonic imaging is performed for geological exploration. Microwave imaging is employed for radar applications. But, the most commonly known imaging systems are visible light imaging. Such systems are employed for applications like remote sensing, microscopy, measurements, consumer electronics, entertainment electronics, etc.

The images acquired by optical, electro-optical or electronic means are likely to be degraded by the sensing environment. The degradation may be in the form of sensor noise, blur due to camera misfocus, relative object camera motion, random atmospheric turbulence, and so on. The noise in an image may be due to a noisy channel if the image is transmitted through a medium. It may also be due to electronic noise associated with a storage-retrieval system.

Noise in an image is a very common problem. An image gets corrupted with noise during acquisition, transmission, storage and retrieval processes. The various types of noise are discussed in the next chapter. Noise may be classified as substitutive noise (impulsive noise: e.g., salt & pepper noise, random-valued impulse noise, etc.) , additive noise (e.g., additive white Gaussian noise) and multiplicative noise(e.g. speckle Noise).The impulse noise of low and moderate noise densities can be removed easily by simple denoising schemes available in the literature. The simple median filter works very nicely for suppressing impulse noise of low density. However, now-a-days, many denoising schemes are proposed which are efficient in suppressing impulse noise of moderate and high noise densities. In many occasions, noise in digital images is found to be additive in nature with uniform power in the whole bandwidth and with Gaussian probability distribution. Such a noise is referred to as Additive White Gaussian Noise (AWGN). It is difficult to suppress AWGN since it corrupts almost all pixels in an image. The arithmetic mean filter, commonly known as Mean filter , can be employed to suppress AWGN but it introduces a blurring effect. Multiplicative (speckle Noise) is an inherent property of medical ultrasound imaging.

Speckle noise occurs in almost all coherent imaging systems such as laser, acoustics and SAR(Synthetic Aperture Radar) imagery. and because of this noise the image resolution and contrast become reduced, thereby reducing the diagnostic value of this imaging modality. So, speckle noise reduction is an important prerequisite, whenever ultrasound imaging is used for tissue characterization. In my work I have introduced this speckle noise to considered image and analysed for various spatial and transform domain filters by considering all the image metrics, which are discussed in chapter 2. Among the many methods that have been proposed to perform this task, there exists a class of approaches that use a multiplicative model of speckled image formation and take advantage of the logarithmical transformation in order to convert multiplicative speckle

noise into additive noise. The common assumption made in a dominant number of such studies is that the samples of the additive noise are mutually uncorrelated and obey a Gaussian distribution. Now the noise became AWGN.

## 1.2 The Problem Statement

Efficient suppression of noise in an image is a very important issue. Denoising finds extensive applications in many fields of image processing. Image Denoising is an important pre-processing task before further processing of image like segmentation, feature extraction, texture analysis etc. The purpose of Denoising is to remove the noise while retaining the edges and other detailed features as much as possible. Conventional techniques of image denoising using linear and nonlinear techniques have already been studied and analyzed for efficient denoising scheme.

In the present work efforts are made to reduce Speckle Noise and AWGN(Additive White Gaussian Noise). Speckle Noise is multiplicative in nature and it occurs in almost all coherent imaging systems such as laser, SAR(Synthetic Aperture Radar) and medical Ultrasound imaging etc...here various Spatial and Transform domain filters are considered to denoise the noisy images, having various noise variances.

## 1.3 Thesis Layout

The thesis is organized as follows. Chapter 2 gives an introduction to various types of noise considered, different metrics used to analyze the efficiency in removing noise from noisy image and literature review. Chapter 3 discusses some linear and non-linear filtering techniques in denoising process. Chapter 4 discusses the recently proposed Circular Spatial Filter(CSF) and adaptive CSF and some other filters. Chapter 5 discusses Wavelet domain filters and application of fuzzy in wavelet domain. chapter 6 discusses conclusion and future work to be done.

## Chapter 2

# Noise in Digital Image

## 2.1 Noise in Digital Images

In this section, various types of noise corrupting an image signal are studied, the sources of various noises are discussed, and mathematical models for these types of noise are shown. Note that noise is undesired information that contaminates the image.

An image gets corrupted with noise during acquisition, transmission, storage and retrieval processes. The various types of noise are discussed in this chapter.

### Additive and Multiplicative Noises

For A efficient denoising technique, information about the type of noise presented in the corrupted image plays a significant role. Mostly images are corrupted with Gaussian, uniform, or salt and pepper distribution noise. Another considerable noise is a speckle noise. Speckle noise is multiplicative noise. The behavior of each of the above mentioned noises is described in Section 2.2.1 through Section 2.2.4

Noise is present in an image either in an additive or multiplicative form

Let the original image  $f(x, y)$  and noise introduced is  $\eta(x, y)$  and the corrupted image be  $w(x, y)$  where  $(x, y)$  gives us the pixel location.

Then, if image gets additive noise then the corrupted image will be

$$w(x, y) = f(x, y) + \eta(x, y) \quad (2.1)$$

Similarly, if multiplicative noise is acquired during processing of image then the corrupted image will be

$$w(x, y) = f(x, y) * \eta(x, y) \quad (2.2)$$

The above two operations will be done at pixel level.

The digital image acquisition process converts an optical image into a electrical signal which is continuous then sampled . At every step in the process there are fluctuations caused by natural phenomena, adding a random value to the given pixel value.

#### 2.1.1 Gaussian Noise

This type of noise adds a random Gaussian distributed noise value to the original pixel value. And it has a Gaussian distribution. It has a bell shaped probability distribution function given by,

$$F(g) = \frac{1}{\sqrt{2\pi\sigma^2}} e^{-(g-m)^2/2\sigma^2} \quad (2.3)$$

where  $g$  represents the gray level,  $m$  is the average or mean of the function, and  $\sigma$  is the standard deviation of the noise. Graphically, it is represented as shown in Figure 2.1.

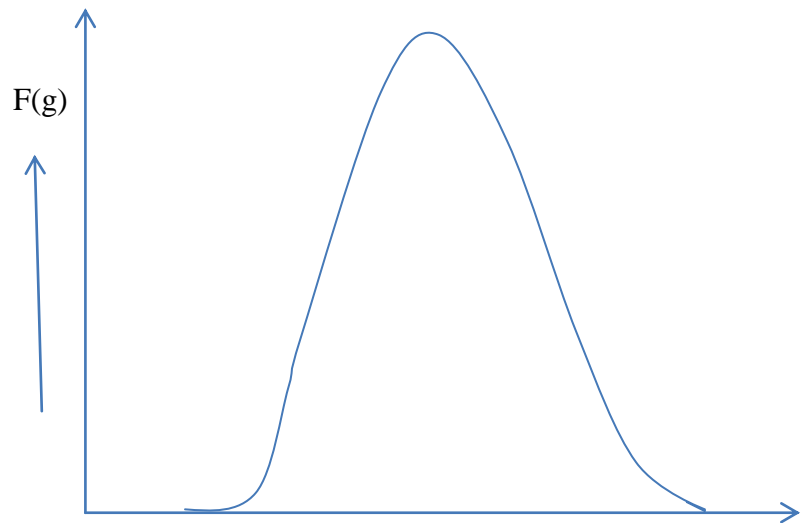


Figure 2.1 Gaussian Noise Distribution

When introduced into an image, Gaussian noise with zero mean and variance as 0.05 would look as in Figure 2.2 which has shown as below.

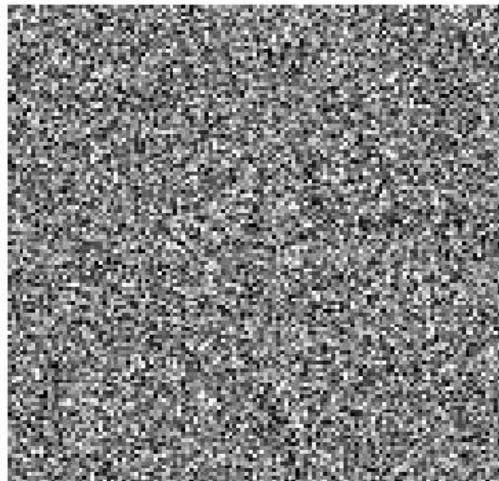


Figure 2.2 Gaussian noise(mean 0, variance 0.05)

### 2.1.2 Salt and Pepper Noise

Salt and pepper noise also called as an impulse noise. It is also referred to as intensity spikes. Mainly while transmitting data we will get this salt and pepper noise. It has only two possible values, 0 and 1. The probability of each value is typically less than 0.1. The corrupted pixel values are set alternatively to the maximum or to the minimum value, giving the image a “salt and pepper” like appearance as salt looks like white (one) and pepper looks as black (zero) for binary ones. Pixels which are not affected by noise remain unchanged. For an 8-bit image, the typical value for pepper noise is 0 (minimum) and for salt noise 255 (maximum). This noise is generally caused in digitization process during timing errors, malfunctioning of pixel elements in the camera sensors, faulty memory locations. The probability density function for Salt and pepper type of noise is shown as below

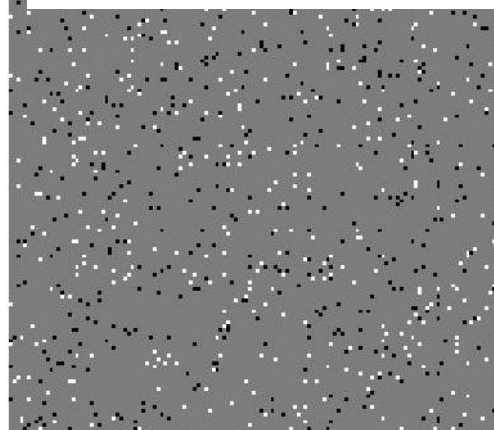
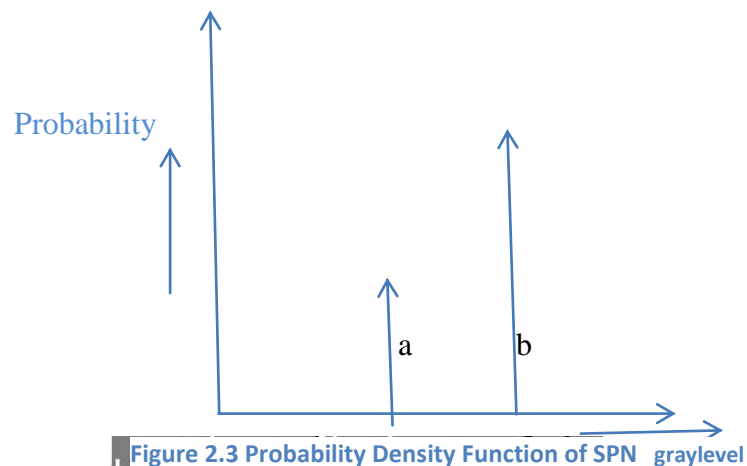


Figure 2.4 salt and pepper noise variance of 0.05

### 2.1.3 Speckle Noise

Speckle Noise is multiplicative in nature. This type of noise usually occurs in almost all coherent imaging systems such as laser, acoustics and SAR(Synthetic Aperture Radar) imagery. This type of noise is an inherent property of medical ultrasound imaging. and because of this noise the image resolution and contrast become reduced, which effects the diagnostic value of this imaging modality. So, speckle noise reduction is an essential preprocessing step, whenever ultrasound imaging is used for medical imaging.

In this thesis, worked mainly on this type of noise along with AWGN noise. Among the many methods that have been proposed to reduce this noise , there exists a class of approaches that use a multiplicative model of speckled image formation and take the advantage of the logarithmical transformation in order to convert multiplicative speckle noise into additive noise with some assumption. The common assumption we have to made in a dominant number of such studies is that the additive noise samples are mutually uncorrelated and these samples obey a Gaussian distribution.

Speckle noise follows a gamma distribution and is given as

$$F(g) = \frac{g^{\alpha-1}}{(\alpha-1)! a^\alpha} e^{-\frac{g}{a}} \quad (2.4)$$

where variance is  $a^2\alpha$  and  $g$  is the gray level.

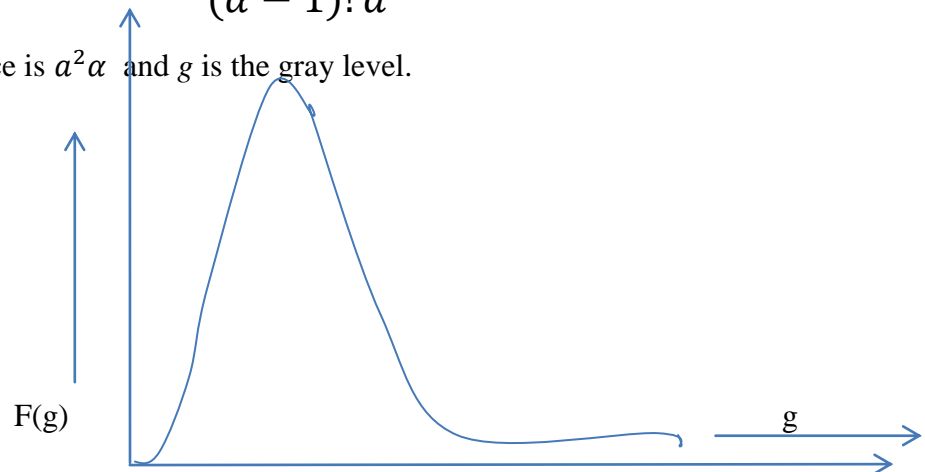


**Figure 2.5 Gamma Distribution**

Speckle noise with variance 0.05 will be as shown below

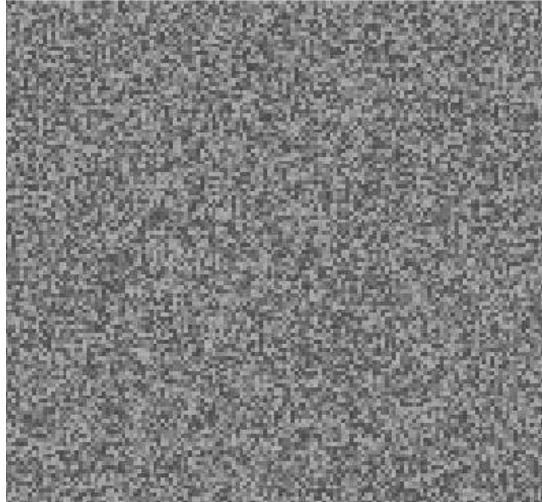


Figure 2.6 Speckle Noise

### 2.1.4 Summary

In this chapter, We have discussed varies types of noise considered in this thesis . By using software we can apply these three above noise(AWGN,salt and pepper and speckle noise) to input images.Among this Speckle noise taken as main noise noise as I worked with medical images.

### 2.2 Image Metrics

The quality of an image is examined by objective evaluation as well as subjective evaluation. For subjective evaluation, the image has to be observed by a human expert. But The human visual system (HVS) is so complicated and this cannot give the exact quality of image.

There are various metrics used for objective evaluation of an image. Some of them are mean square error (MSE), root mean squared error (RMSE), mean absolute error (MAE) and peak signal to noise ratio (PSNR).

Let the original noise-free image  $X(m, n)$ , noisy image  $Y(m, n)$ , and the filtered image be represented  $\tilde{X}(m, n)$  where  $m$  and  $n$  represent the discrete spatial coordinates of the digital images.

Let the images be of size  $M \times N$  pixels, i.e.  $m=1,2,3,\dots,M$ , and  $n=1,2,3,\dots,N$ . Then,

### 2.2.1 Mean Square Error

Mean Square Error (MSE), and Root Mean Squared Error (RMSE) are defined as

$$MSE = \sum_{m=1}^M \sum_{n=1}^N (\tilde{X}(m, n) - X(m, n))^2 \quad (2.5)$$

$$RMSE = \sqrt{MSE} \quad (2.6)$$

Mean Absolute Error is defined as

$$MAE = \sum_{m=1}^M \sum_{n=1}^N |\tilde{X}(m, n) - X(m, n)| \quad (2.7)$$

### 2.2.2 Peak signal to noise ratio (PSNR)

And another important metric is Peak signal to noise ratio (PSNR). It is defined in logarithmic scale, in dB. It is a ratio of peak signal power to noise power. Since the MSE represents the noise power and the peak signal power, the PSNR is defined as:

$$PSNR = 10 * \log_{10} \frac{1}{MSE} \quad (2.8)$$

This image metric is used for evaluating the quality of a filtered image and thereby the capability and efficiency of a filtering process.

In addition to these metrics, universal quality index (UQI) is extensively used to evaluate the quality of an image now-a-days. Further, some parameters, e.g. method noise and execution time are also used in literature to evaluate the filtering performance of a filter. These parameters are discussed below.

### 2.2.3 Universal Quality Index

The universal quality index (UQI) is derived by considering three different factors: (i) loss of correlation, (ii) luminance distortion and (iii) contrast distortion. It is defined by:

$$UQI = \frac{\sigma_f \hat{f}}{\sigma_f \sigma_{\hat{f}}} \cdot \frac{2\bar{f} \bar{\hat{f}}}{(\bar{f})^2 + (\bar{\hat{f}})^2} \cdot \frac{2\sigma_f \sigma_{\hat{f}}}{\sigma_f^2 + \sigma_{\hat{f}}^2} \quad (2.9)$$

Where,

$$\bar{f} = \frac{1}{MXN} \sum_{x=1}^M \sum_{y=1}^N f(x, y) \quad (2.10)$$

$$\bar{\hat{f}} = \frac{1}{MXN} \sum_{x=1}^M \sum_{y=1}^N \hat{f}(x, y) \quad (2.11)$$

$$\sigma_f^2 = \frac{1}{MXN - 1} \sum_{x=1}^M \sum_{y=1}^N (f(x, y) - \bar{f})^2 \quad (2.12)$$

$$\sigma_{\hat{f}}^2 = \frac{1}{MXN - 1} \sum_{x=1}^M \sum_{y=1}^N (\hat{f}(x, y) - \bar{\hat{f}})^2 \quad (2.13)$$

$$\sigma_{f\hat{f}} = \frac{1}{MXN - 1} \sum_{x=1}^M \sum_{y=1}^N (f(x, y) - \bar{f})(\hat{f}(x, y) - \bar{\hat{f}}) \quad (2.14)$$

The UQI defined in (2.9) consists of three components. The first component is the correlation coefficient between the original (noise free) image,  $f$ , and the restored image,  $\hat{f}$ , that measures the degree of linear correlation between them, and its dynamic range is  $[-1, 1]$ . The second component, with a range of  $[0, 1]$ , measures the closeness between the average luminance of  $f$  and  $\hat{f}$ . It reaches the maximum value of 1 if and only if  $f$  equals  $\hat{f}$ . The standard deviations of these two images,  $\sigma_f$  and  $\sigma_{\hat{f}}$  are also used to estimate their contrast-levels. So, the third component in (2.9) is necessarily a measure of the similarity between the contrast-levels of the images. It ranges between 0 and 1 and the optimum value of 1 is achieved only when  $\sigma_f = \sigma_{\hat{f}}$ .

Hence, combining the three parameters: (i) correlation, (ii) average luminance similarity and (iii) contrast-level similarity, the new image metric: universal quality index (UQI) becomes a very good performance measure.

### 2.2.4 Execution Time

Execution Time ( $T_E$ ) of a filter, which is used to reduce noise, is defined as the time taken by a Processor to execute that filtering algorithm when no other software, except the operating system (OS), runs on it.

Execution Time depends essentially on the system's clock time-period, yet it is not necessarily dependant on the clock, memory-size, the input data size, and the memory access time, etc.

The execution time taken by a filtering algorithm should be low for best online and real-time image processing applications. Hence, when all metrics give the identical values then a filter with lower  $T_E$  is better than a filter having higher  $T_E$  value.

### 2.3 Literature Review

In digital imaging, quality of image degrades due to contamination of various types of noise during the process of acquisition, transmission and storage. Noise introduced in an image is usually classified as substitutive (impulsive noise: e.g., salt & pepper noise, random-valued impulse noise, etc.), additive (e.g., additive white Gaussian noise) and multiplicative (e.g., speckle noise). Reducing the noise is very essential tool in medical area also. Among the currently available medical imaging modalities, ultrasound imaging is considered to be best one since it is noninvasive, practically harmless to the human body, portable, accurate, and cost effective. Unfortunately, the quality of medical ultrasound is generally limited because of Speckle noise, which is an inherent property of medical ultrasound imaging, and this noise generally tends to reduce the image resolution and contrast, which reduces the diagnostic value of this imaging modality. So reduction of speckle noise is an important preprocessing step, whenever ultrasound imaging model is used for medical imaging.

Among the many methods that have been proposed to perform this preprocessing task, as we know that speckle noise is multiplicative in nature we can take advantage of the logarithmical transformation in order to convert multiplicative speckle noise into additive noise. The common assumption to be taken here is additive noise samples are mutually uncorrelated and these samples obey a Gaussian distribution. Now the noise became AWGN.

Many spatial-Domain filters such as Mean filter, Median filter, Alpha-trimmed mean filter, Wiener filter, Anisotropic diffusion filter, Total variation filter, Lee filter, Non-local means filter, Bilateral filter etc. are in literature for suppression of AWGN. Also many Wavelet-domain filters such as Visu Shrink, Sure Shrink, Bayes

Shrink,oracle Shrink,Neigh Shrink, Locally adaptive window maximum likelihood estimation etc. are there to suppress the AWGN effectively. Bilateral Filter and the recently devolped filter Circular Spatial Filter (CSF) [4] Performances are comapared with the existing filters in terms of peak-signal-to-noise-ratio (PSNR), root-mean-squared error (RMSE), universal quality index (UQI), and execution time (ET).

### 2.3.1 Bilateral Filter

The Bilateral filter[11] is a nonlinear filter proposed by Tomasi and Manduchi, is used to reduce additive noise from images. Bilateral filtering smooths images while preserving edges, by means of a nonlinear combination of nearby image values. The method is noniterative, local, and simple.

Filtering procedure:

The Bilateral filter kernel,  $w$ , is a product of two sub-kernels

- (i) gray-level kernel,  $w_g$  and
- (ii) distance kernel,  $w_d$ .

Here

Gray level kernel:

The gray-level distance (i.e., photometric distance) between any arbitrary pixel of intensity value  $g(x_1, y_1)$  at location  $(x_1, y_1)$  with respect to its center pixel of intensity value  $g(x, y)$  at location  $(x, y)$  is given by:

$$d_g = [|g^2(x_1, y_1) - g^2(x, y)|]^{\frac{1}{2}} \quad (2.15)$$

The photometric, or gray-level sub-kernel is expressed by:

$$w_g = \exp\left(-\frac{1}{2}\left(\frac{d_g}{\sigma_g}\right)^2\right) \quad (2.16)$$

Where  $\sigma_g$  is the distribution function for  $w_g$ .

distance kernel:

The spatial distance (i.e., geometric distance) between any arbitrary pixel at a location  $(x_1, y_1)$  with respect to the center pixel at location  $(x, y)$  is the Euclidean distance given by:

$$d_s = \sqrt{(x_1 - x)^2 + (y_1 - y)^2} \quad (2.17)$$

The geometric, or distance sub-kernel, is defined by:

$$w_d = \exp\left(-\frac{1}{2}\left(\frac{d_s}{\sigma_d}\right)^2\right) \quad (2.18)$$

Here  $\sigma_d$  is standard deviation of  $w_d$ .

Now, the kernel of bilateral filter is obtained by multiplying equation 2.16 and equation 2.18 and let this kernel be  $w_b$  then

$$w_b = w_g w_d \quad (2.19)$$

Now, to reduce the noise, this kernel should be slide throughout the noisy image and after filtering the estimated output is given below

$$\hat{f}(x, y) = \frac{\sum_{s=-a}^a \sum_{t=-b}^b g(x+s, y+t)}{\sum_{s=-a}^a \sum_{t=-b}^b w_b(s, t)} \quad (2.20)$$

The filter has been used for many applications such as texture removal , dynamic range compression , photograph enhancement. It has also been adapted to other domains such as mesh fairing , volumetric denoising. The large success of bilateral filter is because of various reasons such as its simple formulation and implementation.

### 2.3.2 Circular Spatial Filter(CSF)

In the journal ‘Circular Spatial Filtering under high noise variance condition’ Nilamani Bhoi and Dr. Sukadev Meher proposed a Circular spatial filtering scheme[4]. for suppressing Additive White Gaussian Noise (AWGN) under high noise variance condition. the name circular refers to the shape of the filtering kernel or window being circular. In this method, a circular spatial domain window, whose weights are derived from two independent functions: (i) spatial distance and (ii) gray level distance, is employed for filtering. The weighting function used in gray level kernel for both CSF and bilateral filter are same but the weighting function used in distance kernel of CSF and domain-filtering kernel of Bilateral filter are different. The weighting function used in domain-filtering kernel of Bilateral filter is exponential . But it is a simple nonlinear function in case of distance kernel of the CSF. The CSF filter is performs very well under high noise conditions. It is capable of smoothing Gaussian noise and it is also capable of retaining the detailed information of the image. It gives significant performance in terms of Peak-Signal-to-Noise Ratio (PSNR) and Universal Quality Index (UQI) over many

well known existing methods both in spatial and wavelet domain. The filtered image also gives better visual quality than existing methods.

Filtering procedure:

Let the original image  $f$  be corrupted with additive white Gaussian noise  $\eta$ . Then the corrupted image  $g$  may be expressed as:

$$g(x, y) = f(x, y) + \eta(x, y) \quad (2.21)$$

### Distance kernel

The spatial distance (i.e., geometric distance) between any arbitrary pixel at a location  $(x_1, y_1)$  with respect to the center pixel at location  $(x, y)$  is the Euclidean distance given by:

$$d_s = \sqrt{(x_1 - x)^2 + (y_1 - y)^2} \quad (2.22)$$

Now, the distance kernel is defined as

$$w_d = 1 - \frac{d_s}{d_{max}} \quad (2.23)$$

where  $d_{max}$  is the maximum radial distance from center.

The correlation between pixels goes on decreasing as the distance increases. Hence, when  $w_d$  becomes very small the correlation can be taken as zero. When the small values of distance kernel are replaced by zero we get a circular shaped filtering kernel. The circular shaped kernel is denoted as  $w_{c_d}$ .

### Gray level kernel

The Gray level distance between any arbitrary pixel at a location  $(x_1, y_1)$  with respect to the center pixel at location  $(x, y)$  is the Euclidean distance given by:

$$d_g = [|g^2(x_1, y_1) - g^2(x, y)|]^{\frac{1}{2}} \quad (2.24)$$

The photometric, or gray-level sub-kernel is expressed by:

$$w_g = \exp\left(-\frac{1}{2}\left(\frac{d_g}{\sigma_g}\right)^2\right) \quad (2.25)$$

Where  $\sigma_g$  is the distribution function for  $w_g$ .

Now, by using above two kernel we can get the filtering kernel of CSF can be shown below

$$w_{CSF} = w_{c_d} w_g \quad (2.26)$$

Now, to remove the noise, this kernel should be slide throughout the noisy image and the estimated output after filtering is given below

$$\hat{f}(x, y) = \frac{\sum_{s=-a}^a \sum_{t=-b}^b g(x+s, y+t)}{\sum_{s=-a}^a \sum_{t=-b}^b w_b(s, t)} \quad (2.27)$$

In the filtering window the center coefficient is given highest weight. The weight goes on decreasing as distance increases from center and it is zero when correlation is insignificant. A pictorial representation of circular spatial filtering mask is shown in Fig.2.7.

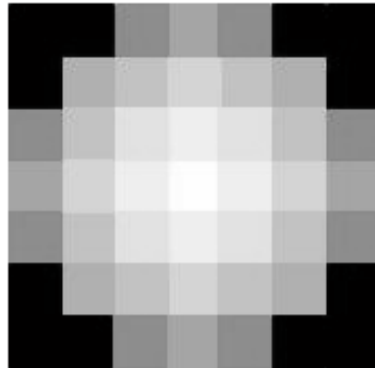


Figure 2.7 circular window for CSF

The selection of window in CSF is equally important as the selection of parameter. The noise levels of AWGN are taken into consideration for selection of window. If there is no a-priori knowledge of the noise level, the robust median estimator is used to find it. For low, moderate and high noise conditions  $3 \times 3$ ,  $5 \times 5$  and  $7 \times 7$  windows are selected respectively for effective suppression of Gaussian noise. The size of the window is kept constant and is never varied even though the image statistics change from point to point for a particular noise level.

### 2.3.3 Adaptive Circular Spatial Filter

the work on CSF is to modify the filter such that this shape of filter should efficiently adaptive so that the all pixels of the image need not be filtered with circular shaped filter, the shape may be semi circular or other shape depends on the location of that pixel or we can also make adaptive the window size of CSF depends on noise variance. where the size of the window varies with the level of complexity of a particular region in an image and the noise power as well. A smooth or flat region (also called as homogenous region) is said to be less complex as compared to an edge region. The region containing edges and textures are treated as highly complex regions. The window size is increased for a smoother region and also for an image with high noise power.

#### Window Selection

The selection of window of adaptive CSF is based on the level of noise present in the considered noisy image.

When the noise level is low ( $\sigma_n \leq 10$ ) then

- i) a  $3 \times 3$  window is selected for filtering the noisy pixels which are belonging to homogenous regions;
- ii) the pixel is not undergo filtering if the noisy pixels belong to edges.

When the noise level is moderate ( $10 < \sigma_n \leq 30$ ),

- i) a  $5 \times 5$  window is chosen for filtration of noisy pixels of flat regions;
- ii) the window size is  $3 \times 3$  if the noisy pixels are edges

When the noise level is high ( $30 < \sigma_n \leq 50$ ),

- i) a  $7 \times 7$  window is used for reducing noise of noisy pixels of flat regions;
- ii) if the noisy pixels to be filtered are edge pixels then  $5 \times 5$  window size should be used.

## 2.4 Simulation Results

Simulation of aforementioned filters are carried out on MatlabR2008a platform. The test images: Lena, Goldhill and Barbara of sizes 512×512 corrupted with AWGN of standard deviation  $\sigma_n = 5, 10, 15, 20, 25, 30, 35, 40, 45, 50, 55, 60, 65, 70, 75, 80$ . and in the similar way medical images: brain, knee, ultrasound baby are considered with Speckle Noise of above mentioned standard deviation values are used for testing the filtering performance. The peak-signal to noise ratio (PSNR), universal quality index (UQI) and execution time are taken as performance measures.

		PSNR(dB)										
		Standard Deviation of AWGN										
Sl.No	Filter Type	5	10	15	20	25	30	35	40	45	50	60
1	Bilateral[3x3]	31.76	31.07	30.06	28.97	27.85	26.83	24.85	24.97	24.20	23.48	22.34
2	Bilateral[5x5]	30.88	29..81	29.50	29.10	28.63	27.83	26.85	25.97	24.20	23.48	22.74
3	Bilateral[7x7]	29.96	27.37	27.26	27.17	26.95	26.73	26.85	26.17	25.20	24.48	23.34
4	CSF[3x3]	36.80	32.75	29.68	27.39	25.52	24.00	22.71	21.59	20.63	19.73	18.76
5	CSF[5x5]	36.80	32.75	29.68	27.39	25.52	24.00	22.71	21.59	20.63	19.73	18.76
6	CSF[7x7]	32.17	31.26	30.44	29.91	29.25	28.61	27.92	27.30	26.96	25.44	24.34
5	Adaptive CSF	32.17	31.26	31.17	30.03	28.30	26.68	24.86	23.16	22.45	20.68	20.35

**Table 2.1 filtering Performance of spatial filters interms of PSNR(dB) operated on Goldhill image.**

		UQI										
		Standard deviation of AWGN										
Sl.No	Filter Type	5	10	15	20	25	30	35	40	45	50	60
1	Bilateral[3x3]	0.9741	0.9732	0.9706	0.9676	0.9646	0.9597	0.9542	0.9475	0.9400	0.9316	0.9306
2	Bilateral[5x5]	0.9734	0.9543	0.9534	0.9520	0.9501	0.9478	0.9447	0.9414	0.9378	0.9329	0.9213
3	Bilateral[7x7]	0.9688	0.9483	0.9477	0.9466	0.9453	0.9436	0.9414	0.9392	0.9386	0.9293	0.9178
4	CSF[3x3]	0.9973	0.9949	0.9849	0.9742	0.9611	0.9452	0.9272	0.9067	0.8854	0.8811	0.8734
5	CSF[5x5]	0.9938	0.9924	0.9900	0.9866	0.9822	0.9771	0.9710	0.9640	0.9555	0.9469	0.9429
6	CSF[7x7]	0.9912	0.9848	0.9839	0.9828	0.9813	0.9789	0.9765	0.9735	0.9700	0.9659	0.9643

**Table 2.2 filtering Performance of spatial filters interms of UQI operated on Goldhill image.**

# Chapter 3

## **Linear and Nonlinear**

## **Filtering**

### 3.1 Background

Filters play a significant role in the image denoising process. It is a technique for modifying or enhancing an image. The basic concept behind reducing noise in noisy images using linear filters is digital convolution and moving window principle. *Linear filtering* is filtering in which the value of an output denoised pixel is a linear combination of the values of the pixels in the input pixel's neighborhood. Let  $w(x)$  be the input signal subjected to filtering, and  $z(x)$  be the filtered output. If the applied filter satisfies certain conditions such as linearity and shift invariance, then the output filter can be expressed mathematically in simple form as given below

$$z(x) = \int w(t)h(x-t)dt \quad (3.1)$$

Where  $h(t)$  is impulse response or point spread function and it completely characterizes the filter. The above process called as convolution and it can be expressed as  $z = w * h$ . In case of discrete convolution the filter is as given below

$$z(i) = \sum_{-\infty}^{\infty} w(t)h(i-t) \quad (3.2)$$

This means that the output  $z(i)$  at point  $i$  is given by a weighted sum of input pixels surrounding  $i$  and here the weights are given by  $h(t)$ . To create the output at the next pixel  $i+1$ , the function  $h(t)$  is shifted by one and the weighted sum is computed again. The overall output is created by a series of shift-multiply-sum operations, and this forms a discrete convolution. For the 2-dimensional case,  $h(t)$  becomes  $h(t,u)$ , and above Equation becomes

$$z(i,j) = \sum_{t=i-k}^{i+k} \sum_{u=j-l}^{j+l} w(t,u)h(i-t,j-u) \quad (3.3)$$

Here the values of  $h(t,u)$  are referred to as the filter weights, the filter kernel, or filter mask. For reasons of symmetry  $h(t,u)$  is always chosen to be of size  $m \times n$  where  $m$  and  $n$  are both usually odd (often  $m=n$ ). In physical systems, always the kernel  $h(t,u)$  must be non-negative, which results in some blurring or averaging of the image. The narrower

the  $h(t, u)$ , then the filter gives less blurring. In digital image processing,  $h(t, u)$  maybe defined arbitrarily and this  $h(t, u)$  gives rise to many types of filters.

## 3.2 Spatial Filters

### 3.2.1 Mean Filter

A mean filter[12] acts on an image by smoothing it. i.e., it reduces the variation in terms of intensity between adjacent pixels. The mean filter is a simple moving window spatial filter, which replaces the center value in the window with the average of all the neighboring pixel values including that centre value. It is implemented with a convolution mask, which provides a result that is a weighted sum of the values of a pixel and its neighbor pixels. It is also called a linear filter. The mask or kernel is a square. Often a  $3 \times 3$  square kernel is used. If the sum of coefficients of the mask equal to one, then the average brightness of the image is not changed. If the sum of the coefficients equal to zero, then mean filter returns a dark image. This average filter works on the shift-multiply-sum principle. This principle in the two-dimensional image can be represented as shown below,

let us consider a  $512 \times 512$  image and  $3 \times 3$  mask and let the filter mask is

$h_1$	$h_2$	$h_3$
$h_4$	$h_5$	$h_6$
$h_7$	$h_8$	$h_9$

Table 3.1  $3 \times 3$  mask

And the neighbourhood of pixel (5,5)

$w_{44}$	$w_{45}$	$w_{46}$
$w_{54}$	$w_{55}$	$w_{56}$
$w_{64}$	$w_{65}$	$w_{66}$

Table 3. 2 neighbourhood of w(5,5)

Then the the output filter value at pixel (5,5) is given as

$$h_1w_{44} + h_2w_{45} + h_3w_{46} + h_4w_{54} + h_5w_{55} + h_6w_{56} + h_7w_{64} + h_8w_{65} + h_9w_{66}$$

In the above filter if all the weights are same then it is called constant weight filter. and If the sum of coefficients of the mask equal to one, then the average brightness of the image is not changed. If the sum of the coefficients equal to zero, the average brightness is lost, and it returns a dark image.for example,here the sum of coefficients equal to one.

$\frac{1}{9}$	$\frac{1}{9}$	$\frac{1}{9}$
$\frac{1}{9}$	$\frac{1}{9}$	$\frac{1}{9}$
$\frac{1}{9}$	$\frac{1}{9}$	$\frac{1}{9}$

Table 3.3 constant weight filter

Computing the straightforward convolution of an image with the above mask carries out the mean filtering process. This mean filter used as a low pass filter, and it does not allow the high frequency components present in the noise. It is to be noted that

larger kernels of size  $5 \times 5$  or  $7 \times 7$  produces more denoising but make the image more blurred. A tradeoff is to be made between the kernel size and the amount of denoising.

### 3.2.2 Median Filter

A median filter[17] comes under the class of nonlinear filter. It also follows the moving window principle, like mean filter. A  $3 \times 3$ ,  $5 \times 5$ , or  $7 \times 7$  kernel of pixels is moved over the entire image. First the median of the pixel values in the window is computed, and then the center pixel of the window is replaced with the computed median value. Calculation of Median is done as first sorting all the pixel values from the surrounding neighborhood(either ascending or descending order) and then replacing the pixel being considered with the middle pixel value.

The below process illustrates the methodology of median filtering

Let us take  $3 \times 3$  mask and the pixel values of image in the neighbourhood of considered noisy pixel are

125	147	175	111	150
120	115	150	108	118
122	132	<b>140</b>	107	112
112	152	128	134	112
134	155	155	198	145

Table 3.4 median values in the neighbourhood of 140

Let us consider pixel at (3,3) i.e., pixel value of 100. Neighbourhood of this pixel are 115,150,108,132,107,152,128,134.

After sorting these pixels(in ascending order) we will get

107,108,115,128,132,134,140,150,152.

And the median value among this is 132(5<sup>th</sup> value). So, now this pixel magnitude 140 will replace with the value of 132 unrepresentative of the surrounding pixels.

The median is more robust compared to the mean. Since one of the neighbour value or considered pixel used as median, this filter does not create new pixel values

when the filter straddles an edge. It shows that median filter preserves sharp edges than the mean filter.

### 3.2.3 Wiener Filter

The Wiener filter[12] is a spatial-domain filter and it generally used for suppression of additive noise. Norbert Wiener proposed the concept of Wiener filtering in the year 1942. There are two methods: (i) Fourier-transform method (frequency-domain) and (ii) mean-squared method (spatial-domain) for implementing Wiener filter. The Fourier method is used only for denoising and deblurring, whereas the latter is used for denoising. In Fourier transform method of Wiener filtering requires a priori knowledge of the noise power spectra and the original image. But in latter method no such a priori knowledge is required. Hence, it is easier to use the mean-squared method for development. Wiener filter is based on the least-squared principle, i.e. the this filter minimizes the mean-squared error (MSE) between the actual output and the desired output.

Image statistics vary too much from a region to another even within the same image. Thus, both global statistics (mean, variance, etc. of the whole image) and local statistics (mean, variance, etc. of a small region or sub-image) are important. Wiener filtering is based on both the global statistics and local statistics and is given

$$\hat{f}(x, y) = \bar{g} + \frac{\sigma_f^2}{\sigma_f^2 + \sigma_\eta^2} (g(x, y) - \bar{g}) \quad (3.4)$$

Where  $\hat{f}(x, y)$  denotes the restored image,  $\bar{g}$  is the local mean,  $\sigma_f^2$  is the local variance and  $\sigma_\eta^2$  is the noise variance.

Let us consider  $(2m+1) \times (2n+1)$  window then local mean  $\bar{g}$  is defined as

$$\bar{g} = \frac{1}{L} \sum_{s=-m}^m \sum_{t=-n}^n g(s, t) \quad (3.5)$$

where,  $L$ , is the total number of pixels in a window.

Similarly, consider  $(2m+1) \times (2n+1)$  window then local variance  $\sigma_g^2$  is defined as

$$\sigma_g^2 = \frac{1}{L-1} \sum_{s=-m}^m \sum_{t=-n}^n (g(s, t) - \bar{g})^2 \quad (3.6)$$

The local signal variance,  $\sigma_f^2$  is used in (3.4) is calculated from  $\sigma_g^2$  with a priori knowledge of noise variance,  $\sigma_n^2$  simply by subtracting  $\sigma_n^2$  from  $\sigma_g^2$  with the assumption that the signal and noise are not correlated with each other.

From (3.4) it may be observed that the filter-output is equal to local mean, if the current pixel value equals local mean. Otherwise, it outputs a different value. the value being some what different from local mean. If the input current value is more (less) than the local mean, then the filter outputs a positive (negative) differential amount taking the noise variance and the signal variance into consideration. Thus, the filter output varies from the local mean depending upon the local variance and hence tries to catch the true original value as far as possible. In statistical theory, Wiener filtering is a great landmark. It estimates the original data with minimum mean-squared error and hence, the overall noise power in the filtered output is minimal. Thus, it is accepted as a benchmark in 1-D and 2-D signal processing

### 3.2.4 Lee Filter

The Lee filter[6] , developed by Jong-Sen Lee, is an adaptive filter which changes its characteristics according to the local statistics in the neighborhood of the current pixel. The Lee filter is able to smooth away noise in flat regions, but leaves the fine details (such as lines and textures) unchanged. It uses small window ( $3 \times 3$ ,  $5 \times 5$ ,  $7 \times 7$ ). Within each window, the local mean and variances are estimated.

The output of Lee filter at the center pixel of location  $(x, y)$  is expressed as:

$$\hat{f}(x, y) = k(x, y)[g(x, y) - \bar{g}] + \bar{g} \quad (3.7)$$

where

$$k(x, y) = \begin{cases} 1 - \frac{\sigma_n^2}{\sigma_g^2} & \sigma_g^2 > \sigma_n^2 \\ 0 & \sigma_g^2 \leq \sigma_n^2 \end{cases} \quad (3.8)$$

The parameter  $k(x, y)$  ranges between 0 (for flat regions) and 1 (for regions with high signal activity). The distinct characteristic of the filter is that in the areas of low

signal activity (flat regions) the estimated pixel approaches the local mean, whereas in the areas of high signal activity (edge areas) the estimated pixel favours the corrupted image pixel, thus retaining the edge information. It is generally claimed that human vision is more sensitive to noise in a flat area than in an edge area. The major drawback of the filter is that it leaves noise in the vicinity of edges and lines. However, it is still desirable to reduce noise in the edge area without sacrificing the edge sharpness. Some variants of Lee filter available in the literature handle multiplicative noise and yield edge sharpening.

### 3.2.5 Anisotropic Diffusion (AD) Filter

In order to be able to identify global objects through blurring, it is necessary to extract a family of derived images of multiple scales of resolution. and that this may be viewed equivalently as the solution of the heat conduction or diffusion equation given by

$$g_t = C \cdot \nabla^2 g \quad (3.9)$$

where,  $g_t$  is the first derivative of the image  $g$  in time  $t$ ,  $\nabla^2$  is the Laplacian operator with respect to space variables and  $C$  is the constant which is independent of space location. Koenderink considered it so because it simplifies the analysis greatly. Perona and Malik developed a smoothing scheme based on anisotropic diffusion filtering[6] that overcomes the major drawbacks of conventional spatial smoothing filters and improves the image quality significantly.

Perona and Malik considered the anisotropic diffusion equation as:

$$\begin{aligned} g_t &= \frac{\partial g(x, y, t)}{\partial t} = \text{div}(C(x, y, t) \cdot \nabla g(x, y, t)) \\ &= C(x, y, t) \nabla^2 g + \nabla C \cdot \nabla g \end{aligned} \quad (3.10)$$

Where  $\text{div}$  is the divergence and  $\nabla$  is the gradient operator with space variables. By taking  $C(x, y, t)$  be a constant, (3.10) reduces to (3.9), the isotropic diffusion equation.

Perona and Malik considered the image gradient as an estimation of edges and  $= U(\nabla g)$ , in which  $U(\cdot)$  has to be a nonnegative monotonically decreasing function with  $U(0) = 1$  (in the interval of uniform region) and tends to zero at infinity. There are some possible choices for  $U(\cdot)$ , the obvious being a binary valued function. Some other functions could be:

$$U(s) = \exp\left[-\frac{|s|^2}{k^2}\right] \quad (3.11)$$

It can also denotes as given below

$$U(s) = \frac{1}{1 + \left[\frac{|s|}{k}\right]^2} \quad (3.12)$$

Here  $k$  is the threshold value which is very important factor in removing noise. Equation (3.10) can be discretized using four nearest neighbors (north, south, east, west) and the Laplacian operator and it is given by

$$g^{n+1}(x, y) = g^n(x, y) + \lambda[(C_N \cdot \nabla_N g(x, y) + C_S \cdot \nabla_S g(x, y) + C_W \cdot \nabla_W g(x, y) + C_E \cdot \nabla_E g(x, y))]^2 \quad (3.13)$$

Here  $g^{n+1}(x, y)$  is the discrete value of  $g(x, y)$  in the  $(n+1)^{\text{th}}$  iteration which is set by  $n$  as  $g$  is determined by  $t$  in continuous space.  $g^{n+1}(x, y)$  the given equations

$$C_N = U(|\nabla_N g(x, y)|) \quad (3.14)$$

$$\nabla_N g(x, y) = g(x - 1, y) - g(x, y) \quad (3.15)$$

$$C_S = U(|\nabla_S g(x, y)|) \quad (3.16)$$

$$\nabla_S g(x, y) = g(x + 1, y) - g(x, y) \quad (3.17)$$

$$C_W = U(|\nabla_W g(x, y)|) \quad (3.18)$$

$$\nabla_W g(x, y) = g(x, y - 1) - g(x, y) \quad (3.19)$$

$$C_E = U(|\nabla_E g(x, y)|) \quad (3.20)$$

$$\nabla_E g(x, y) = g(x, y + 1) - g(x, y) \quad (3.21)$$

And  $\lambda$  is used for stability and then the filtered image is given by  $\widehat{f}(x, y) = g^{n+1}(x, y)$

### 3.2.6 Total Variation (TV) Filter

Rudin et al. proposed Total variation (TV). It is a constrained optimization type of numerical algorithm for denoising the noisy images. The total variation of the image is minimized subject to constraints involving the statistics of the affected noise. The constraints are imposed using Lagrange multipliers. Here we are using the gradient-projection method. This amounts to solving a time dependent partial differential equation on a manifold determined by the constraints. As  $t \rightarrow \infty$  the solution converges to a steady state which is the denoised image.

In total variation algorithm, the gradients of noisy image,  $g(x,y)$  in four directions (East, West, North and South) are calculated. The gradients in all four directions are calculated as follows.

$$\nabla_N g(x, y) = g(x - 1, y) - g(x, y) \quad (3.22)$$

$$\nabla_S g(x, y) = g(x + 1, y) - g(x, y) \quad (3.23)$$

$$\nabla_W g(x, y) = g(x, y - 1) - g(x, y) \quad (3.24)$$

$$\nabla_E g(x, y) = g(x, y + 1) - g(x, y) \quad (3.25)$$

Where  $\nabla$  is the gradient operator.

The noisy image undergoes several iterations to suppress AWGN through TV filter. The resulted output image after (n+1) iterations is expressed as:

$$\begin{aligned} & \tilde{g}^{n+1}(x, y) \\ &= \tilde{g}^n(x, y) \\ &+ \frac{\Delta t}{h} \left[ \nabla_N \left( \frac{\nabla_S \tilde{g}^n(x, y)}{\sqrt{\nabla_S \tilde{g}^n(x, y) + (m(\nabla_E \tilde{g}^n(x, y), \nabla_W \tilde{g}^n(x, y)))^2}} \right) \right. \\ &+ \left. \nabla_W \left( \frac{\nabla_E \tilde{g}^n(x, y)}{\sqrt{\nabla_E \tilde{g}^n(x, y) + (m(\nabla_S \tilde{g}^n(x, y), \nabla_N \tilde{g}^n(x, y)))^2}} \right) \right] \\ &- \Delta t \lambda^n (\tilde{g}^n(x, y) - g(x, y)) \end{aligned} \quad (3.26)$$

Where,

$$\begin{aligned}
 m(a, b) &= \min \text{mod} (a, b) \\
 &= \left[ \frac{\text{sgn } a + \text{sgn } b}{2} \right] \min(|a|, |b|)
 \end{aligned} \tag{3.27}$$

Where

$\text{sgn } x$  is 1 for  $x \geq 0$  and it is 0  $x < 0$ .

And  $\lambda$  is a controlling parameter,  $\Delta t$  is the discrete time-step and  $h$  is a constant.

A restriction, imposed for stability, is given by:

$$\frac{\Delta t}{h^2} \leq c \quad \text{here } c \text{ is constant.}$$

The filtered image is then  $\hat{f}(x, y) = \tilde{g}^{n+1}(x, y)$ .

### 3.3 Simulation Results

The filters which are mentioned in this chapter are simulated on MatlabR2008a platform and the results are shown below.

		PSNR(dB)												
		Standard deviation of AWGN( $\sigma_n$ )												
S.No	Filter Type	5	10	15	20	25	30	35	40	45	50	60	70	80
1	Mean[3x3]	30.24	29.12	28.97	27.74	26.49	25.19	24.89	24.53	23.13	22.82	22.23	21.13	20.63
2	Mean[5x5]	26.08	26.05	26.01	25.97	25.89	25.83	25.76	25.67	25.57	25.46	25.24	24.95	24.38
3	Mean[7x7]	25.69	24.68	23.66	23.64	23.61	23.59	23.54	23.50	23.46	23.40	23.31	23.21	23.05
4	Median[3x3]	33.76	30.44	28.78	27.22	25.90	24.67	23.61	22.65	21.77	21.02	20.19	19.87	18.45
5	Median[5x5]	30.77	28.60	27.96	27.32	26.63	25.95	25.32	24.66	24.01	23.43	22.45	21.76	20.98
6	Median[7x7]	29.34	27.29	26.95	26.62	26.19	25.78	25.43	24.99	24.67	24.20	23.87	22.34	21.89
7	Wiener[3x3]	36.63	32.35	30.41	28.59	26.96	25.62	24.41	23.32	22.47	21.62	19.89	18.87	18.10
8	Wiener[5x5]	34.88	30.43	29.56	28.67	27.76	26.88	26.00	25.17	24.45	23.68	22.76	21.89	20.87
9	Wiener[7x7]	32.99	28.87	28.31	27.67	27.08	26.51	25.89	25.26	24.71	24.07	23.09	22.12	21.90
10	Lee [3x3]	36.60	32.38	30.03	28.31	26.96	25.86	24.85	23.98	23.21	22.58	21.09	20.19	19.89
11	Lee[5x5]	36.29	32.00	29.95	28.59	27.65	26.87	26.12	25.49	24.93	24.51	23.22	21.98	20.18
12	Lee[7x7]	35.98	31.56	29.48	28.22	27.32	26.62	26.05	25.59	25.15	24.69	22.89	21.98	20.98
13	Anisotropic Diffusion	33.07	29.88	29.13	28.27	27.38	26.50	25.65	24.83	24.06	23.40	22.65	21.89	20.00
14	Total Variation	33.11	31.30	30.19	29.13	28.09	27.16	26.27	25.41	24.62	23.71	22.10	21.89	20.09

**Table3. 5 PSNR (dB) values of denoised image of MRI Brain using various filters under various standard deviation**

		UQI									
No	Filter type	Standard deviation of AWGN( $\sigma_n$ )									
1	Mean[3x3]	0.9939	0.9928	0.9909	0.9884	0.9850	0.9809	0.9763	0.9705	0.9643	0.9567
2	Mean[5x5]	0.9866	0.9861	0.9853	0.9841	0.9827	0.9807	0.9784	0.9754	0.9722	0.9677
3	Mean[7x7]	0.9801	0.9799	0.9793	0.9785	0.9777	0.9762	0.9744	0.9722	0.9698	0.9567
4	Median[3x3]	0.9945	0.9922	0.9866	0.9838	0.9781	0.9710	0.9631	0.9542	0.9444	0.9344
5	Median[5x5]	0.9916	0.9880	0.9860	0.9839	0.9812	0.9780	0.9746	0.9631	0.9542	0.9444
6	Median[7x7]	0.9878	0.9838	0.9824	0.9810	0.9790	0.9769	0.9747	0.9723	0.9654	0.9567
7	Wiener[3x3]	0.9971	0.9950	0.9880	0.9860	0.9839	0.9812	0.9780	0.9746	0.9631	0.9542
8	Wiener[5x5]	0.9942	0.9921	0.9903	0.9838	0.9824	0.9810	0.9790	0.9769	0.9747	0.9654
9	Wiener[7x7]	0.9917	0.9886	0.9848	0.9838	0.9824	0.9810	0.9790	0.9769	0.9631	0.9542
10	Lee [3x3]	0.9981	0.9950	0.9921	0.9903	0.9838	0.9824	0.9810	0.9790	0.9769	0.9747
11	Lee[5x5]	0.9956	0.9916	0.9862	0.9837	0.9819	0.9797	0.9774	0.9735	0.9665	0.9456
12	Lee[7x7]	0.9958	0.9936	0.9924	0.9903	0.9838	0.9824	0.9819	0.9797	0.9774	0.9735
13	Anisotropic Diffusion	0.9957	0.9936	0.9924	0.9878	0.9846	0.9776	0.9687	0.9624	0.9567	0.9514
14	Total Variation	0.9954	0.9941	0.9911	0.9876	0.9845	0.9810	0.9789	0.9720	0.9623	0.9623

**Table3. 6 UQI values of denoised image of MRI Brain using various filters under various standard deviation**

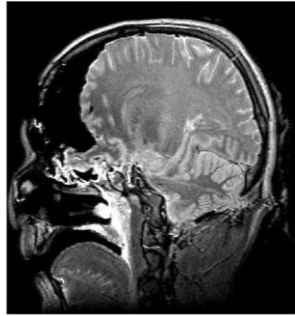
		PSNR(dB)												
		Standard deviation of Speckle Noise( $\sigma_n$ )												
S.No	Filter Type	5	10	15	20	25	30	35	40	45	50	60	70	80
1	Mean[3x3]	30.12	29.67	29.24	28.49	27.19	26.89	25.53	24.13	23.82	23.23	23.13	22.63	22.34
2	Mean[5x5]	26.45	26.11	25.77	25.91	25.83	25.76	25.57	24.57	25.46	25.24	24.95	24.38	23.45
3	Mean[7x7]	23.68	23.66	23.64	23.61	23.59	23.54	23.50	23.46	23.40	23.31	23.21	23.05	22.34
4	Median[3x3]	30.44	28.78	27.22	25.90	24.67	23.61	22.65	21.77	21.02	20.19	19.87	18.45	17.87
5	Median[5x5]	28.60	27.96	27.32	26.63	25.95	25.32	24.66	24.01	23.43	22.45	21.76	20.98	18.98
6	Median[7x7]	27.29	26.95	26.62	26.19	25.78	25.43	24.99	24.67	24.20	23.87	22.34	21.89	20.89
7	Wiener[3x3]	32.35	30.41	28.59	26.96	25.62	24.41	23.32	22.47	21.62	19.89	18.87	18.10	17.65
8	Wiener[5x5]	30.43	29.56	28.67	27.76	26.88	26.00	25.17	24.45	23.68	22.76	21.89	20.87	19.28
9	Wiener[7x7]	28.87	28.31	27.67	27.08	26.51	25.89	25.26	24.71	24.07	23.09	22.12	21.90	20.89
10	Lee [3x3]	32.38	30.03	28.31	26.96	25.86	24.85	23.98	23.21	22.58	21.09	20.19	19.89	17.99
11	Lee[5x5]	32.00	29.95	28.59	27.65	26.87	26.12	25.49	24.93	24.51	23.22	21.98	20.18	18.76
12	Lee[7x7]	31.56	29.48	28.22	27.32	26.62	26.05	25.59	25.15	24.69	22.89	21.98	20.98	18.76
13	Anisotropic Diffusion	29.88	29.13	28.27	27.38	26.50	25.65	24.83	24.06	23.40	22.65	21.89	20.00	18.76
14	Total Variation	31.30	30.19	29.13	28.09	27.16	26.27	25.41	24.62	23.71	22.10	21.89	20.09	18.65

**Table3. 7 PSNR (dB) values of denoised image of MRI Brain using various filters under various standard deviation**

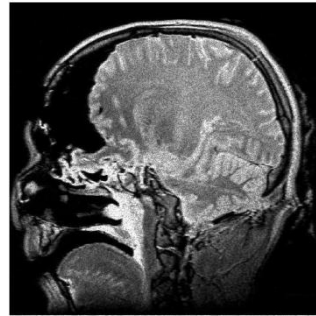
		UQI									
No	Filter type	Standard deviation of Speckle Noise( $\sigma_n$ )									
		5	10	15	20	25	30	35	40	45	50
1	Mean[3x3]	0.9919	0.9878	0.9859	0.9814	0.9790	0.9709	0.9683	0.9605	0.9583	0.9567
2	Mean[5x5]	0.9886	0.9861	0.9843	0.9811	0.9787	0.9717	0.9684	0.9654	0.9622	0.9617
3	Mean[7x7]	0.9801	0.9799	0.9793	0.9785	0.9777	0.9762	0.9744	0.9722	0.9698	0.9567
4	Median[3x3]	0.9985	0.9932	0.9876	0.9838	0.9781	0.9710	0.9631	0.9542	0.9444	0.9344
5	Median[5x5]	0.9912	0.9870	0.9862	0.9853	0.9802	0.9780	0.9746	0.9611	0.9542	0.9444
6	Median[7x7]	0.9878	0.9838	0.9824	0.9810	0.9790	0.9769	0.9747	0.9723	0.9654	0.9567
7	Wiener[3x3]	0.9971	0.9950	0.9880	0.9860	0.9839	0.9812	0.9780	0.9746	0.9631	0.9542
8	Wiener[5x5]	0.9952	0.9931	0.9913	0.9838	0.9824	0.9810	0.9790	0.9769	0.9747	0.9654
9	Wiener[7x7]	0.9917	0.9886	0.9858	0.9842	0.9824	0.9810	0.9790	0.9769	0.9631	0.9542
10	Lee [3x3]	0.9971	0.9951	0.9923	0.9913	0.9838	0.9824	0.9810	0.9790	0.9769	0.9747
11	Lee[5x5]	0.9958	0.9926	0.9872	0.9837	0.9819	0.9797	0.9774	0.9735	0.9685	0.9456
12	Lee[7x7]	0.9958	0.9936	0.9924	0.9903	0.9828	0.9814	0.9819	0.9797	0.9784	0.9735
13	Anisotropic Diffusion	0.9957	0.9936	0.9924	0.9878	0.9836	0.9746	0.9657	0.9624	0.9577	0.9514
14	Total Variation	0.9971	0.9951	0.9872	0.9837	0.9819	0.9767	0.9678	0.9645	0.9564	0.9522

**Table3. 7 UQI values of denoised image of MRI Brain using various filters under various standard deviation**

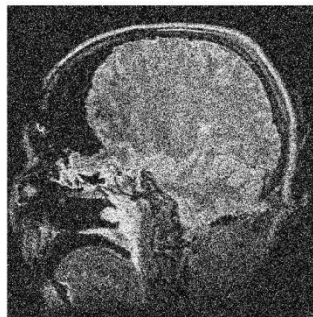
Performance of spatial domain filters on MRI brain image under standard deviation of 25 of speckle noise.



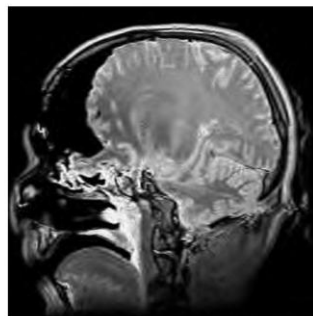
Original image



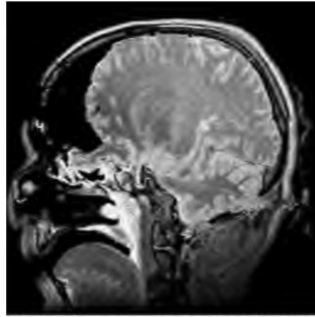
Noisy image of Noise variance 25



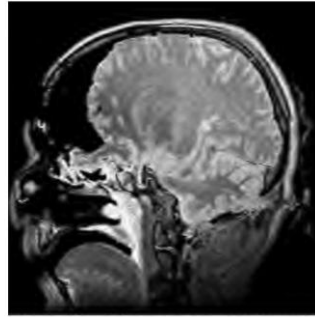
Noisy image at  $\sigma_n = 45$



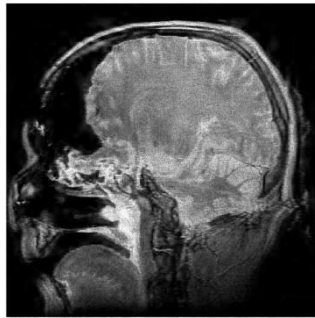
Filtered image Using Mean Filter



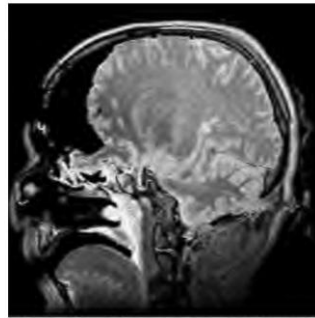
Filtered image using Lee[7x7]



Filtered image using wiener[5x5]



Filtered image using AD



Filtered image using TV

# Chapter 4

# Wavelet Domain Filtering

## 4.1 Discrete Wavelet Transform (DWT)

Wavelets are simply mathematical functions and these functions analyze data according to scale or resolution. They aid in studying a signal at different resolutions or in different windows. The wavelet transform was borne out of a need for further developments from Fourier transforms. Wavelets transform signals in the time domain (rather, assumed to be in the time domain) to a joint time-frequency domain. The main weakness that was found in Fourier transforms was their lack of localized support, which made them susceptible to Heisenberg's Uncertainty principle. In short, this means that we could get information about the frequencies present in a signal, but not where and when the frequencies occurred. Wavelets, on the other hand, are not anywhere as subject to it. Wavelets provide some more advantages over Fourier transforms. For example, they do a better job in approximating signals with sharp spikes or signals having discontinuities whereas fourier transform doesnot give efficient results. Mainly, Wavelets can be used in image compression, turbulence, radar, human vision, earthquake prediction, etc.

A wavelet is, as the name might suggest, a little piece of a wave. The finite scale multiresolution representation of a discrete function can be known as a discrete wavelet transform (DWT).It is a fast linear operation on a data vector, whose length is an integer power of 2. Discrete wavelet transform is invertible and orthogonal, where the inverse transform expressed as a matrix is the transpose of the transform matrix. The wavelet basis or wave let function is quite localized in space. But individual wavelet functions are localized in frequency similar to sines and cosines in fourier transform. The orthonormal basis or wavelet basis is defined as

$$\Psi_{(j,k)}(x) = 2^{j/2}\psi(2^j x - k) \quad (4.1)$$

And the scaling function is given as

$$\phi_{(j,k)}(x) = 2^{j/2}\phi(2^j x - k) \quad (4.2)$$

Where  $\Psi$  is wavelet function and  $j$  and  $k$  are integers that scale and dilate the wavelet basis or function. The factor 'j' in the above equations is known as the scale index and it indicates the wavelet's width. The factor 'k' provides the position. The wavelet function is dilated by powers of two and it is translated by the integer  $k$ . In terms of the wavelet coefficients, the wavelet equation is

$$\Psi(x) = \sum_k^{N-1} g_k \sqrt{2\phi(2x - k)} \quad (4.3)$$

Here  $g_0, g_1, g_2, \dots$  are high pass wavelet coefficients.

Scaling equation in terms of the scaling coefficients is given as shown below,

$$\phi(x) = \sum_k^{N-1} h_k \sqrt{2\phi(2x - k)} \quad (4.4)$$

Where the function  $\phi(x)$  is scaling function and the coefficients  $h_0, h_1, h_2, \dots$  are low pass coefficients.

The wavelet and scaling coefficients are related by quadrature mirror relationship as given below

$$g_n = (-1)^n h_{1-n+N} \quad (4.5)$$

Where N is the number of vanishing moments.

The wavelet equation produces different types of wavelet families like Daubechies, Haar, symlets, coiflets, etc. . Wavelets are classified into a family by the number of vanishing moments  $N$ . Within each family of wavelets there are wavelet subclasses distinguished by the number of coefficients and by the level of iterations.

Wavelet Family	Filters Length	Number Of Vanishing Moments,N
Haar	2	1
Daubechies M	2M	M
Coiflets	6M	2M-1
Symlets	2M	M

**Table 4.1 Wavelet families and their properties**

## 4.2 Properties of DWT

Some of the properties of discrete wavelet transforms (DWT) are listed below

- i) DWT is a fast linear operation, which can be applied on data vectors having length as integer power of 2.
- ii) The wavelet basis is quite localized in space as well as in frequency

- iii) DWT is invertible and orthogonal. Note that the scaling function  $\phi$  and the wavelet function  $\Psi$  are orthogonal to each other in  $L^2(0,1)$ , i.e.,  $\langle \phi, \Psi \rangle = 0$ .
- iv) The scaling coefficients satisfy some constraints

$$\sum_{i=0}^{2N-1} h_i = \sqrt{2}$$

$$\sum_{i=0}^{2N-1} h_i h_{i+2l} = \delta_{1,0} \quad \text{here } l \text{ is the location index, } \delta \text{ is}$$

the delta function and N is the number of vanishing moments.

- v) Wavelet coefficients almost exhibit decorrelation property as given below

$$E[g_j(k)g_{j'}(k')] \approx |2^{-j}k - 2^{-j}k'|^{2(H-N)} \quad (4.6)$$

Where N is the number of vanishing moments and H is the hurst parameter for fractional Brownian motion (fBm).

- vi) The wavelet coefficients of a fractional Brownian motion (fBm) supports Stationarity, i.e.,  $g_j(K) = g_j(0), \forall k$ .

Wavelet coefficients exhibit Gaussianity as  $g_j(k) \sim N(0, \sigma_\Psi 2^{2jH})$  where H is the hurst parameter for fractional Brownian motion (fBm) and  $\sigma_\Psi$  is a constant depending on  $\Psi$ .

The above Gaussianity property exhibited by wavelets used in denoising images corrupted with additive Gaussian noise. The decorrelation exhibited by the wavelet coefficients is also important because it explains a Karhunen-Loeve-like expansion that is implicitly performed for  $1/f$  processes using orthogonal wavelet bases.

### 4.3 Wavelet Thresholding

Donoho and Johnstone have done the lot of work on filtering of additive Gaussian noise using wavelet thresholding. Wavelets play a major role in image compression and image denoising. These Wavelet coefficients calculated by a wavelet transform represent change in the time series at a particular resolution. By considering the time series at various resolutions, it is then possible to filter out the noise.

After applying wavelet transform small coefficients are dominated by noise, while coefficients with a large absolute value carry more signal information than noise. Replacing the smallest, noisy coefficients by zero and a backwards wavelet transform on

the result may lead to a reconstruction with the essential signal characteristics and with less noise. For thresholding three observations and assumptions:

1. The decorrelating property of a wavelet transform creates a sparse signal: most untouched coefficients are zero or close to zero.
2. Noise is spread out equally over all coefficients.
3. The noise level is not too high, so that we can recognize the signal and the signal wavelet coefficients.

So, choosing of threshold level is important task. the coefficients having magnitude greater than threshold are considered as signal of interest and keep the same or modified according to type of threshold selected and other coefficients become zero. The image is reconstructed from the modified coefficients. This process is also known as the inverse discrete wavelet transform (IDWT).

Selection of threshold is an important point of interest. Care should be taken so as to preserve the edges of the denoised image. There exist various methods for wavelet thresholding, which rely on the choice of a threshold value. Some typically used methods for denoising image are Visu Shrink, Sure Shrink, Bayes Shrink, Neigh shrink, oracle Shrink, Smooth Shrink and Fuzzy based Shrink.

Prior to the discussion of these above methods, it is important to know about the two general categories of thresholding. They are hard- thresholding and soft-thresholding types.

The hard-thresholding  $T_H$  can be defined as

$$T_H = \begin{cases} x & \text{for } |x| > t \\ 0 & \text{in all other regions} \end{cases}$$

Here  $t$  is threshold value. plot for this is as shown below

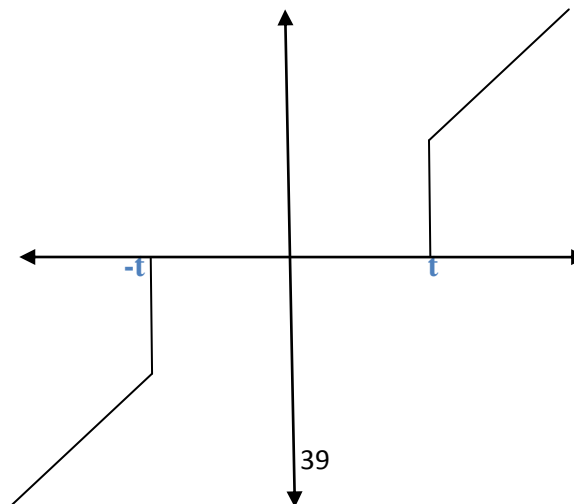


Figure 4.1 Hard Thresholding

In This, all coefficients whose magnitude is greater than the selected threshold value  $t$  remain same and the others whose magnitude is smaller than  $t$  are set to zero. It creates a region around zero where the coefficients are considered negligible.

In Soft thresholding [5] , The coefficients whose magnitude is greater than the selected threshold value are become shrinks towards zero and others set to zero .

The Soft-thresholding  $T_S$  can be defined as

$$T_S = \begin{cases} \text{sign}(x)(|x| - t) & \text{for } |x| > t \\ 0 & \text{in all other regions} \end{cases}$$

Plot as shown below,

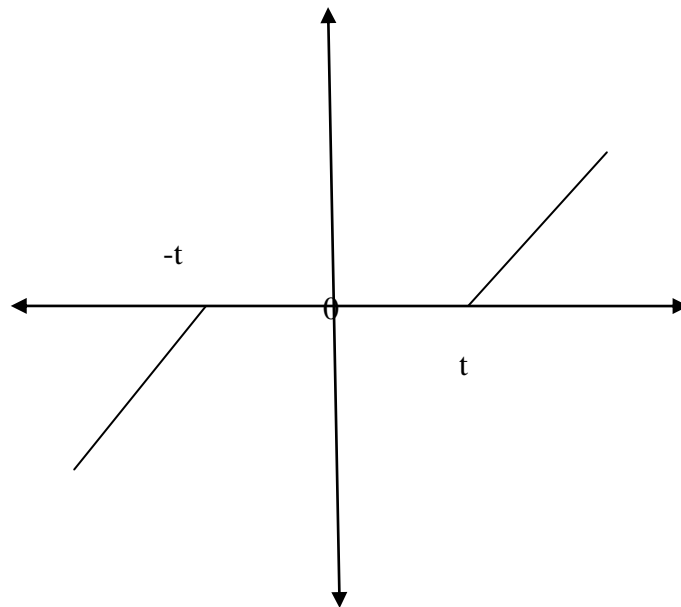


Figure 4.2 Soft Thresholding

In practice, it can be seen that the soft method is much better and yields more visually pleasant images. This is because the hard method is discontinuous and yields abrupt artifacts in the recovered images. Also, the soft method yields a smaller minimum mean squared error compared to hard form of thresholding.

Now let us focus on the all methods of thresholding mentioned earlier. For all

these methods the image is first subjected to a discrete wavelet transform, which decomposes the image into various sub-bands.

Graphically wavelet decomposition is shown as below,

LL3	HL3	HL2	HL1
HL3	HH3		
LH2		HH2	HH1
LH1			

Table 4.2 2-D WAVELET DECOMPOSITION

The sub-bands  $HHk, HLk, LHk, k = 1, 2, \dots, J$  are called the details, where  $K$  is the scale and  $J$  denotes the largest or coarsest scale in decomposition. Note,  $LLk$  is the low resolution component. Thresholding is now applied to the detail components of these sub bands to remove the unwanted coefficients, which contribute to noise. And as a final step in the denoising algorithm, the inverse discrete wavelet transform is applied to build back the modified image from its coefficients.



Figure 4.3 Two level decomposition of lenna image

## 4.4 Types of Wavelet Denoising

### 4.4.1 VisuShrink

VisuShrink was introduced by Donoho . the threshold value „t“ in this type is derived from the standard deviation of the noise. It uses hard thresholding rule. It is also called as universal threshold and is defined as

$$t = \sigma \sqrt{2 \log n} \quad (4.7)$$

$\sigma^2$  is the noise variance present in the signal and  $n$  represents the signal size or number of samples. An estimate of the noise level  $\sigma$  was defined based on the median absolute deviation given by

$$\hat{\sigma} = \frac{\text{median}(\{|g_{j-1,k}| : k = 0,1, \dots, 2^{j-1} - 1\})}{0.6745} \quad (4.8)$$

Where  $g_{j-1,k}$  is refers to the detail coefficients in the wavelet transform.

The main drawback of VisuShrink is it does not deal with minimizing the mean squared error . However, VisuShrink gives the images that are overly smoothed. This is because VisuShrink removes too many coefficients. Another disadvantage is that it cannot remove speckle noise, which is multiplicative noise. It can only deal with an additive noise. VisuShrink follows the global thresholding scheme, here global threshold means a single value of threshold applied globally to all the wavelet coefficients.

#### 4.4.2 SureShrink

A threshold chooser based on Stein's Unbiased Risk Estimator (SURE) was proposed by Donoho and Johnstone and is called as SureShrink. It is determined from the both universal threshold and the SURE threshold. It is subband dependent threshold. A threshold value for each resolution level in the wavelet transform which is referred to as level dependent thresholding. The main advantage of SureShrink is to minimize the mean squared error, unlike Visu Shrink, defined as

$$MSE = \frac{1}{n^2} \sum_{x,y=1}^n (z(x,y) - s(x,y))^2 \quad (4.9)$$

where  $z(x,y)$  is the estimate of the signal while  $s(x,y)$  is the original signal without noise

and  $n$  is the size of the signal. SureShrink suppresses noise by thresholding the empirical wavelet coefficients. The SureShrink threshold  $t_s$  is defined as

$$t_s = \min(t, \sigma\sqrt{2 \log n}) \quad (4.10)$$

where  $t$  denotes the value that minimizes Stein's Unbiased Risk Estimator,  $\sigma$  is the noise variance computed, and  $n$  is the size of the image. It follows the soft thresholding rule. The thresholding employed here is adaptive, i.e., a threshold level is assigned to each resolution level by the principle of minimizing the Stein's Unbiased Risk Estimator for threshold estimates. It is smoothness adaptive i.e., if the unknown function contains abrupt changes or boundaries in the image, the reconstructed image also does.

#### 4.4.3 BayesShrink

BayesShrink was proposed by Chang, Yu and Vetterli. The goal of this method is to minimize the Bayesian risk, and hence its name, BayesShrink. It uses soft thresholding and it is also subband-dependent, like Sure Shrink, which means that threshold level is selected at each band of resolution in the wavelet decomposition. The Bayes threshold,  $t_b$ , is defined as

$$t_b = \frac{\sigma^2}{\sigma_s} \quad (4.11)$$

where  $\sigma^2$  is the noise variance and  $\sigma_s^2$  is the signal variance without noise. The noise variance  $\sigma^2$  is estimated from the subband HH1 in the decomposition of wavelet by the median estimator.. From the definition of additive noise we have

$$w(x, y) = s(x, y) + \eta(x, y) \quad (4.12)$$

Since the signal and noise are independent of each other it can be stated that

$$\sigma_w^2 = \sigma_s^2 + \sigma^2$$

$\sigma_w^2$  can be calculated as shown below

$$\sigma_w^2 = \frac{1}{n^2} \sum_{x,y=1}^n w^2(x, y) \quad (4.13)$$

The variance of the signal,  $\sigma^2$  is computed as shown below

$$\sigma_s = \sqrt{\max(\sigma_w^2 - \sigma^2, 0)} \quad (4.14)$$

With these  $\sigma^2$  and  $\sigma_w^2$  the Bayes threshold is computed from the below equation

$$t_b = \frac{\sigma^2}{\sigma_s} \quad (4.15)$$

the wavelet coefficients are thresholded at each band

#### 4.4.4 OracleShrink

OracleShrink is wavelet thresholding method Used in image denoising. This method is implemented with the assumption that the wavelet coefficients of original decomposed image are known. The OracleShrink uses the threshold denoted as  $T_{OS}$  Mathematically they are represented by:

$$T_{OS} = \arg \min_{T_h} \sum_{i,j=1}^n (\xi_{T_h}(Y_{ij}) - F_{ij})^2 \quad (4.16)$$

Here,  $\{F_{ij}\}$  are wavelet coefficients of the original decomposed image.

$\xi_{T_h}(\cdot)$  is the softthresholding function and  $\zeta_{T_h}(\cdot)$  is hard thresholding function

$$\xi_T(x) = \text{sgn}(x) \cdot \max(|x| - T, 0) \quad (4.18)$$

and

$$\zeta_T(x) = x \cdot 1_{\{|x| > T\}} \quad (4.19)$$

equation 4.19 keeps the input if it is larger than the threshold  $T$  ; otherwise, it is set to zero.

#### 4.4.5 NeighShrink

This wavelet-domain image thresholding scheme was proposed by Chen *et al.* and it incorporating neighboring coefficients, namely NeighShrink. It thresholds the wavelet coefficients according to the magnitude of the squared sum of all the wavelet coefficients, i.e., the local energy, within the neighborhood window. The neighborhood window size may be  $3 \times 3, 5 \times 5, 7 \times 7, 9 \times 9$ , etc. The shrinkage function for *NeighShrink* of any arbitrary  $3 \times 3$  window centered at  $(i, j)$  is expressed as:

$$\Gamma_{ij} = \left[ 1 - \frac{T_U^2}{S_{ij}^2} \right]_+ \quad (4.20)$$

Where  $T_U$  is the universal threshold and  $S_{ij}^2$  is the squared sum of all wavelet coefficients in the given window.

$$\text{i.e.,} \quad S_{ij}^2 = \sum_{n=j-1}^{j+1} \sum_{m=i-1}^{i+1} Y_{m,n}^2 \quad (4.21)$$

here very important consideration is '+' sign at the end of the formula it means keep the positive values while setting it to zero when it is negative.

The estimated center wavelet coefficient  $\hat{F}_{ij}$  is then calculated from its noisy counterpart  $Y_{ij}$  as:

$$\hat{F}_{ij} = \Gamma_{ij} \cdot Y_{ij} \quad (4.22)$$

#### 4.4.6 Smooth Shrink

It is a wavelet-domain image denoising method, proposed by Mastriani *et al.* This is mainly used to reduce Speckle noise. It uses a convolution kernel based on a directional smoothing (DS) function. After applying DWT the aforementioned kernel is applied on the wavelet coefficients. Here window size is adaptive. It also gives good results for additive noise.

#### SmoothShrink Algorithm

Step 1:

The average of the wavelet coefficients in four directions (d1, d2, d3, d4) as shown in Table 4.3 is calculated.

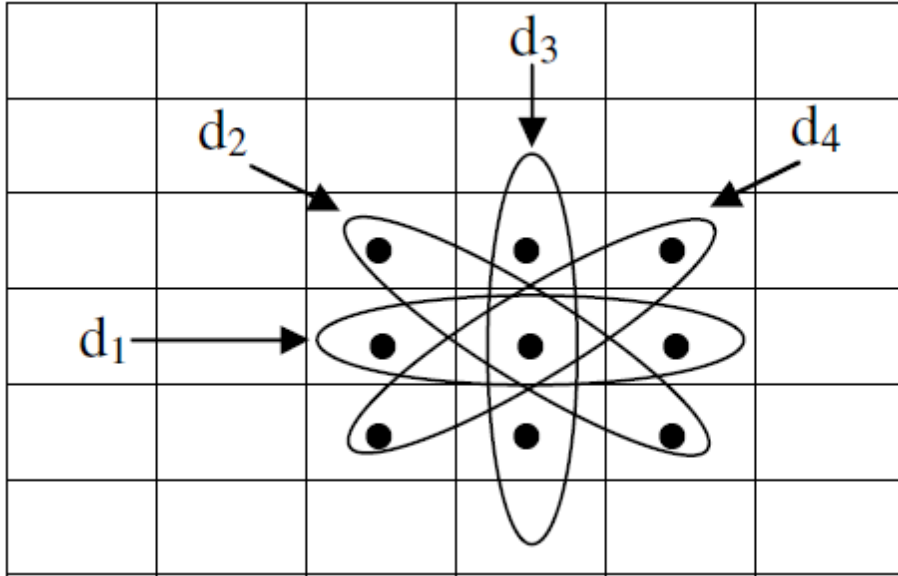


Table 4.3 3X3 directional window

Step 2:

Let  $\bar{Y}_{d_n}$  is average of wavelet coefficients in  $n^{\text{th}}$  direction.

Then the absolute difference between centre wavelet coefficient and each directional average is

$$\Delta d_n = |\bar{Y}_{d_n} - Y_{ij}| \quad (4.23)$$

Step 3 :

The directional average which gives minimum absolute difference is given below.

$$\mathcal{K} = \arg \min_{\bar{Y}_{d_n}} (\{\Delta d_n\}) \quad (4.24)$$

Step 4:

The estimated center wavelet coefficient is therefore replaced with the minimum directional average obtained in Step-3, i.e.

$$\hat{F}_{ij} = \mathcal{K} \quad (4.25)$$

## 4.5 Fuzzy based Wavelet Shrinkage

### 4.5.1 Introduction of fuzzy Logic

A fuzzy system is represented by fuzzy variables that are members of a fuzzy set. A fuzzy set is a generalization of a classical set based on the concept of partial membership. Let  $F$  be a fuzzy set defined on universe of discourse  $U$ . The fuzzy set is described by the membership  $\mu_F(u)$  that maps  $U$  to the real interval  $[0,1]$  i.e. the membership  $\mu$  varying from 0 to 1: a membership of value 0 signifying the fact that the element  $\mu \in U$  does not belong to the set  $F$ ; a membership of value 1 signifying that the element  $\mu \in U$  belongs to the set  $F$  with full certainty; a membership of any other value from 0 to 1 representing the element  $u$  to be a partial member of the set  $F$ . Fuzzy sets are identified by linguistic labels e.g. low, medium, high, very high, tall, very tall, cool, hot, very hot, etc. The knowledge of a human expert can very well be implemented, in an engineering system, by using fuzzy rules.

Fuzzy image filters are already proposed by many researchers for suppressing various types of noises mentioned in chapter 2. Simple fuzzy based filters are proposed using triangular membership function as shown in Fig. 4.4. The membership equals zero at some minimum and maximum gray values of the pixels in the neighborhood of the center pixel under consideration.

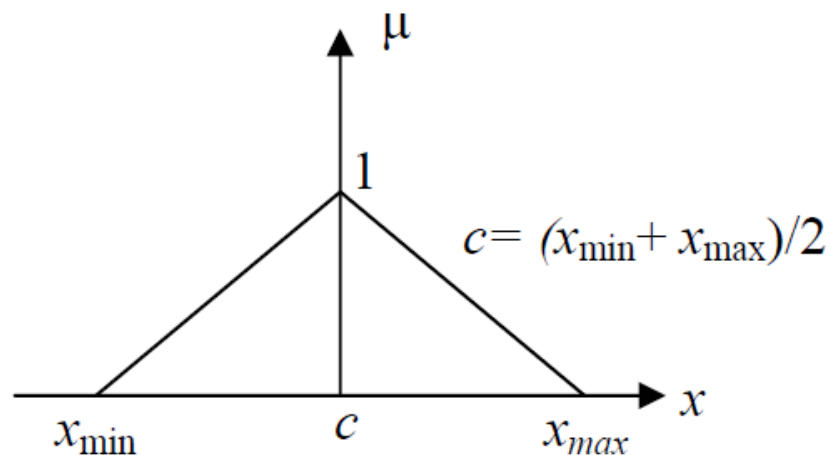


Figure 4.4 Triangular membership function

## 4.5.2 Procedure for fuzzy based wavelet shrinkage denoising

### technique[16]

the usage of fuzzy set theory in the domain of image enhancement using wavelet thresholding. Since we are using Fuzzy Logic the execution will be reduced. It reduces the adaptive Gaussian noise from noisy images.

However, algorithms those derived on the basis of dependencies between the wavelet coefficients can give the better reduction of noise performance, compared with the ones using an independence assumption. The wavelet coefficients are statistically dependent mainly due to two properties of the wavelet transform of natural images: (1) large coefficients will propagate across the scales (interscale dependencies), and (2) if a coefficient is large/small, some of the neighbouring coefficients are also likely to be large/small (intrascale dependencies).

After taking a particular threshold value, If a certain wavelet coefficient and its neighbouring coefficients are small enough we know that this coefficient is noisy one. Coefficients above a certain threshold contain the most important details and we can consider them as signal of interest. but coefficients with values around the threshold contain both noise and signals of interest. A good threshold is generally chosen so that most coefficients below the threshold are noise and values above the threshold are signals of interest. In such situation it can be advantageous to use fuzzy set theory as kind of soft-threshold method. Fuzzy set theory is a mathematical extension of the binary set theory. Fuzzy set theory and fuzzy logic offer us powerful tools to represent and process human knowledge represented as fuzzy if-then rules. Fuzzy image processing has three main stages:

- (i) image fuzzification,
- (ii) modification of membership values and
- (iii) image defuzzification. The fuzzification and defuzzification steps are due to the fact that we do not yet possess fuzzy hardware. Therefore, the coding of image data (fuzzification) and decoding of the results (defuzzification) are steps that make it possible

to process images with fuzzy techniques. The main power of fuzzy image processing lies in the second step (modification of membership values). After the image data is transformed from input plane to the membership plane (fuzzification), appropriate fuzzy techniques modify the membership values. This can be a fuzzy clustering, a fuzzy rule-based approach, a fuzzy integration approach, etc.

The main advantages of the this fuzzy method are:

- (i) execution time is less.
- (ii) we do not lose any noise reduction performance and
- (iii) by adding new fuzzy rules it should be easily extendable to incorporate other information as well.

Here we are considering two parameters

- (i) Considered wavelet coefficient and let it be  $w_{s,d}(i, j)$  where  $s$  and  $d$  gives scale and orientation
- (ii) The local spatial activity indicator was defined as the average magnitude of the surrounding wavelet coefficients within a local window, and it is given by

And let the threshold be  $\sigma$  and if the wavelet coefficient has magnitude greater than  $\sigma$  then it is signal of interest and if it is less than or equal to threshold value then it is considered as noise.

$$x_{s,d}(i, j) = \frac{(\sum_{k=-K}^K \sum_{l=-K}^K |w_{s,d}(i+k, j+l)|) - w_{s,d}(i, j)}{(2K+1)^2 - 1} \quad (4.26)$$

### Fuzzy Rule

The definition of signal of interest is

- IF ( $|x_{s,d}(i, j)|$  is a large variable and  $|w_{s,d}(i, j)|$  is a large coefficient )  
 OR  $|x_{s,d}(i, j)|$  is a large variable  
 THEN  $w_{s,d}(i, j)$  is a signal of interest.

### Membership Function

In many image processing methods it is important that each filtering method is adapted to the noise situation (noise level). Therefore we have related all these parameters to the standard deviation of the noise. Good choices for the parameters are:

$T1 = \sigma$ ,  $T2 = 2\sigma$  and  $T3 = 2.9\sigma - 2.625$ , where  $\sigma$  is the standard deviation of the noise, which is estimated with the median estimator proposed by Donoho and Johnstone. Those threshold values were obtained experimentally by optimising their performance on several test images with several noise levels.

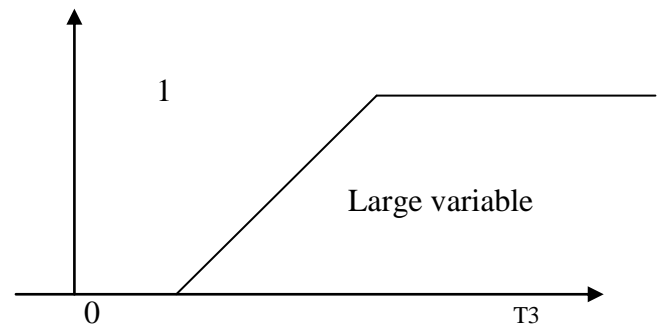
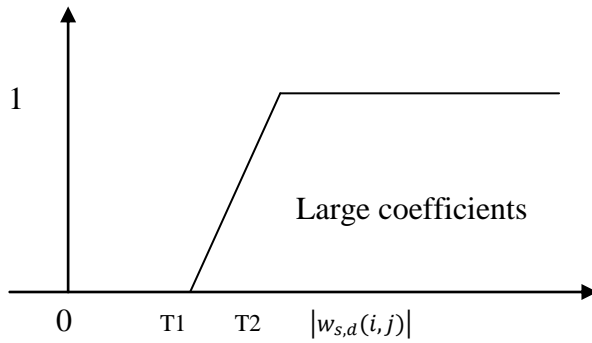


Figure 4.5 membership function for large coefficient    Figure 4.6 membership function for large variable ( $|x_{s,d}(i,j)|$ )

Let membership function for large coefficient be  $\mu_w$  and membership function for large variable be  $\mu_x$

Then the degree of activation is defined as

$$\begin{aligned} \gamma(w_{s,d}(i,j), x_{s,d}(i,j)) \\ = \alpha + \mu_x(|x_{s,d}(i,j)|) - \alpha \cdot \mu_x(|x_{s,d}(i,j)|) \end{aligned} \quad (4.27)$$

Where

$$\alpha = \mu_x(|x_{s,d}(i,j)|) \cdot \mu_w(|w_{s,d}(i,j)|)$$

The value obtained from eq(4.27) gives the membership degree in the fuzzy set signal of interest for the wavelet coefficient. If the membership degree has value 1, this means that the corresponding coefficient is a signal of interest certainly (and should not be changed), while a degree zero indicates that the coefficient is certainly not a signal of interest (and should be set equal to zero). A value between zero and one indicates that we do not know quite sure if this coefficient is a signal of interest or not. This means that the coefficient is a signal of interest only to a certain degree.

## 4.6 Simulation Results

Denoising of images using Visu Shrink, Sure Shrink, Bayes Shrink, neigh shrink, Oracle Shrink, Smoothshrink and Fuzzy based Wavelet Shrinkage filter are discussed in this chapter. All these methods are based on the application of wavelet transforms. Each of these methods is compared in terms of the peak signal to noise ratio, Universal Quality Index as shown below. And execution time of different methods on 3 different systems are noted down.

Above filters are simulated on Matlab R2008a platform. The test images goldhill, brain, ultrasound(baby) image. These images are of size 512x512 and corrupted with AWGN and Speckle of standard deviation  $\sigma_n = 5, 10, 15, 20, 25, 30, 35, 40, 45, 50, 60, 70$  are used for simulation purpose. The peak-signal-to-noise ratio (PSNR), universal quality index (UQI) and execution time are taken as performance measures. Let us consider image of brain. Comparison in terms of PSNR is noted in Table 4.4 and Table 4.5, for AWGN of different standard deviations are considered.

Sl. No		PSNR(dB)											
		Standard Deviation of AWGN( $\sigma_n$ )											
		5	10	15	20	25	30	35	40	45	50	60	70
1	Visu Shrink	29.71	28.64	27.74	26.93	25.91	24.84	23.70	22.47	21.35	20.26	20.69	19.76
2	Sure Shrink	25.36	25.22	24.97	24.60	24.16	23.69	23.20	22.66	22.15	21.63	20.69	19.76
3	Bayes Shrink	36.98	32.44	29.93	28.03	26.30	24.68	23.86	23.16	22.45	21.68	20.35	19.85
4	Neigh Shrink	37.86	33.14	30.45	28.57	27.12	25.92	24.82	23.92	23.11	22.41	21.12	20.14
5	Oracle Shrink	33.86	29.22	26.03	24.68	23.12	21.78	20.75	19.79	18.93	18.11	17.11	16.12
6	Smooth Shrink	25.09	24.78	23.78	22.35	21.47	23.85	19.54	18.56	18.16	17.67	17.12	16.87
7	Fuzzy based	30.23	29.24	28.94	28.14	27.45	25.83	25.16	23.98	22.65	22.34	21.21	19.14

**Table 4.4 filtering Performance of Wavelet Domain filters in terms of PSNR(dB) operated on MRI image of Brain**

## Wavelet Domain filters

		Peak Signal to Noise Ratio, PSNR(dB)											
		Standard Deviation of Speckle Noise( $\sigma_n$ )											
Sl. No	Filter Type	5	10	15	20	25	30	35	40	45	50	60	70
1	Visu Shrink	27.57	26.89	26.35	25.74	25.31	24.73	24.01	23.29	22.02	21.82	20.31	18.96
2	Sure Shrink	25.41	25.39	25.35	25.32	25.29	25.17	25.11	25.02	24.89	24.77	24.57	24.08
3	Bayes Shrink	38.81	35.33	31.78	27.78	26.85	26.42	25.87	24.91	23.87	23.53	23.37	22.93
4	Neigh Shrink	40.82	36.85	34.34	31.98	30.39	29.45	28.71	28.02	27.40	26.86	25.88	25.07
5	Oracle Shrink	41.35	36.99	32.07	29.96	28.47	27.14	26.17	25.28	24.87	23.79	23.20	22.08
6	Smooth Shrink	25.08	24.88	24.70	24.45	24.15	23.83	23.48	23.11	22.75	22.37	22.02	21.21
7	Fuzzy based	39.56	35.23	31.65	28.89	25.67	24.56	23.14	22.10	20.45	20.11	19.87	19.24

**Table 4.5 filtering Performance of Wavelet Domain filters in terms of PSNR(db) operated on MRI image of Brain**

		Universal Quality Index(UQI)									
		Standard deviation of Speckle ( $\sigma_n$ )									
Sl. No	Filter Type	5	10	15	20	30	35	45	50	60	70
1	Visu Shrink	0.9881	0.9861	0.9842	0.9819	0.9773	0.9733	0.9635	0.9561	0.9377	0.8987
2	Sure Shrink	0.9800	0.9799	0.9797	0.9795	0.9787	0.9784	0.9772	0.9765	0.9749	0.9723
3	Bayes Shrink	0.9991	0.9980	0.9954	0.9884	0.9842	0.9820	0.9712	0.9686	0.9656	0.9612
4	Neigh Shrink	0.9994	0.9982	0.9968	0.9953	0.9922	0.9907	0.9874	0.9857	0.9819	0.9811
5	Oracle Shrink	0.9995	0.9979	0.9958	0.9931	0.9867	0.9834	0.9754	0.9710	0.9607	0.9587
6	Smooth Shrink	0.9773	0.9767	0.9757	0.9743	0.9704	0.9679	0.9622	0.9587	0.9467	0.9324
7	Fuzzy based	0.9919	0.9867	0.9837	0.9812	0.9786	0.9761	0.9640	0.9621	0.9543	0.9489

**Table 4.6 filtering Performance of Wavelet Domain filters in terms of UQI operated on MRI image of Brain**

		Peak Signal to Noise Ratio, PSNR(dB)													
		Standard Deviation of Speckle Noise( $\sigma_n$ )													
Sl.No	Filter Type	5	10	15	20	25	30	35	40	45	50	60	70	80	
1	Visu Shrink	31.03	30.32	30.01	29.65	24.76	23.20	22.66	21.85	20.78	19.77	17.80	16.59	14.98	
2	Sure Shrink	30.13	29.43	29.13	28.96	28.76	28.40	28.10	27.83	27.19	27.10	26.09	26.66	17.08	
3	Bayes Shrink	38.28	32.03	30.88	29.44	28.81	28.33	28.08	27.79	<b>27.42</b>	<b>27.01</b>	25.84	25.58	25.21	
4	Neigh Shrink	<b>40.56</b>	<b>35.87</b>	<b>33.23</b>	<b>31.88</b>	30.76	29.45	28.64	27.98	27.00	26.89	<b>25.99</b>	25.02	24.43	
5	Oracle Shrink	40.37	34.36	32.12	31.33	30.85	29.40	28.34	27.57	26.96	26.16	24.29	22.53	20.98	
6	Smooth Shrink	28.75	28.48	28.08	27.58	27.03	26.98	25.86	25.25	24.67	24.09	23.04	22.06	21.19	
7	Fuzzy based	34.34	33.45	31.23	29.89	28.12	27.89	27.78	26.90	26.56	24.53	24.09	23.98	23.43	

**Table 4.7 Filtering Performance of Wavelet Domain filters in terms of PSNR(dB) operated on ultrasound image of baby**

		Universal Quality Index(UQI)									
		Standard deviation of AWGN ( $\sigma_n$ )									
Sl. No	Filter Type	5	10	15	20	30	35	45	50	60	70
1	Visu Shrink	0.9898	0.9878	0.9776	0.9678	0.9587	0.9478	0.9412	0.9324	0.9289	0.9134
2	Sure Shrink	0.9796	0.9787	0.9772	0.9748	0.9719	0.9685	0.9644	0.9578	0.9432	0.9343
3	Bayes Shrink	0.9986	0.9961	0.9813	0.9674	0.9291	0.9055	0.8533	0.8232	0.8156	0.8117
4	Neigh Shrink	0.9989	0.9967	0.9937	0.9902	0.9816	0.9761	0.9640	0.9621	0.9543	0.9489
5	Oracle Shrink	0.9972	0.9917	0.9847	0.9755	0.9512	0.9387	0.9036	0.8851	0.8798	0.8565
6	Smooth Shrink	0.9760	0.9720	0.9656	0.9570	0.9339	0.9198	0.9035	0.8890	0.8798	0.8677
7	Fuzzy based	0.9888	0.9815	0.9786	0.9710	0.9675	0.9567	0.9435	0.9365	0.9267	0.9112

**Table 4.8 filtering Performance of Wavelet Domain filters in terms of UQI operated on MRI image of Ultrasound baby**

As mentioned in chapter 2, Speckle Noise is inherent property in medical images, which is multiplicative in nature. Table 4.6 and Table 4.7 are given the comparison among various wavelet filters in terms of PSNR and UQI metrics. Test image is MRI brain image. Now let us consider Ultrasound baby image to remove the noise.

		Universal Quality Index(UQI)									
		Standard deviation of Speckle ( $\sigma_n$ )									
Sl. No	Filter Type	5	10	15	20	30	35	45	50	60	70
UQI_ IN		0.9994	0.9974	0.9968	0.9944	0.9878	0.9831	0.9728	0.9667	0.9527	0.9375
1	Visu Shrink	0.9903	0.9885	0.9877	0.9866	0.9556	0.9509	0.9294	0.9137	0.8703	0.8107
2	Sure Shrink	0.9853	0.9851	0.9849	0.9842	0.9833	0.9813	0.9810	0.9806	0.9793	0.9761
3	Bayes Shrink	0.9982	0.9923	0.9898	0.9858	0.9836	0.9816	0.9805	0.9771	0.9666	0.9642
4	Neigh Shrink	<b>0.9994</b>	<b>0.9982</b>	<b>0.9968</b>	<b>0.9953</b>	<b>0.9922</b>	<b>0.9907</b>	0.9874	0.9857	0.9819	0.9811
5	Oracle Shrink	0.9989	0.9952	0.9924	0.9903	0.9867	0.9834	0.9754	0.9710	0.9607	0.9587
6	Smooth Shrink	0.9929	0.9819	0.9801	0.9776	0.9704	0.9679	0.9622	0.9587	0.9467	0.9324
7	Fuzzy based	0.9953	0.9921	0.9899	0.9858	0.9836	0.9816	0.9771	0.9666	0.9642	0.9567

**Table 4.9 filtering Performance of Wavelet Domain filters in terms of UQI operated  
On ultrasound image of baby**

Execution time is another important image metric to compare the performance of filter. These wavelet domain filters are simulated using matlab R2008a platform on two different systems having different operating systems, one has(system 1) 64-bit operating system windows vista having intel core(TM)2duo CPU @2.40GH and having RAM of 2015MB. another one (system2) has 64- windows 7 having intel core i3 CPU having RAM 3GB.

**Table 4.10 Execution time of wavlet domain filters**

Denoising filter	Execution Time(secs)	
	System1	System2
Visu Shrink	3.87	2.45
Sure Shrink	4.21	3.56
Bayes Shrink	11.54	8.45
Neigh Shrink	25.22	18.34
Oracle Shrink	8.98	6.89
Smooth Shrink	6.98	5.78
Fuzzy based	6.65	4.45

So, if we consider Execution time as image metric here visu Shrink has low value i.e., visu Shrink is best filter among these but it doesnot has good values in terms of PSNR and UQI, where as Neigh Shrink is best in terms of PSNR and UQI but it doesnot has better Execution time value. Here Fuzzy based wavelet filter gives moderate values in both PSNR, UQI and Execution time .

Performance of wavelet filters on MRI brain image ,which contaminated by speckle noise of standard deviation of 45

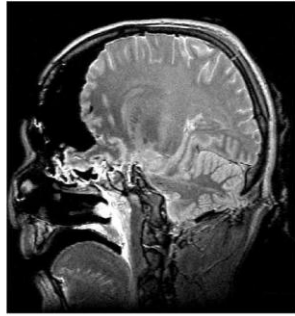


Figure4.8 Original image

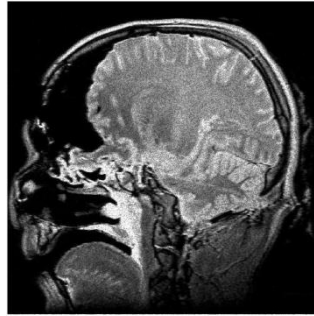


Figure 4.9 Noisy image of Noise variance 25

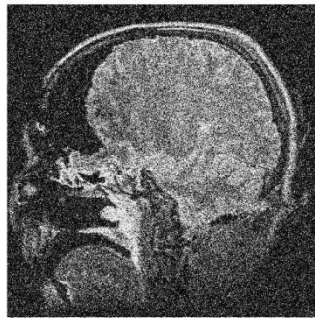


Figure 4.10 Noisy image at  $\sigma_n = 45$



Figure 4.11 Denoised image using VisuShrink

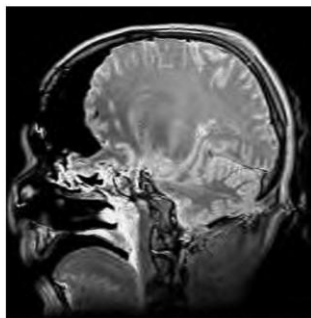


Figure 4,12 Denoised imageUsing Sure Shrink

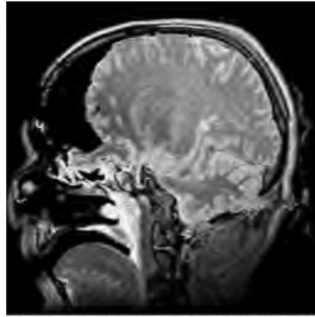


Figure 4.13 Denoised using Bayes Shrink

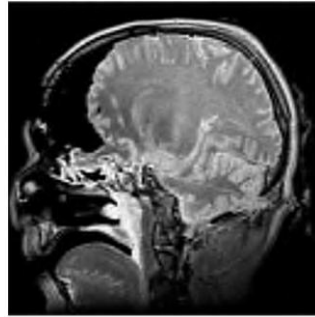


Figure 4.14 Denoised Neigh Shrink

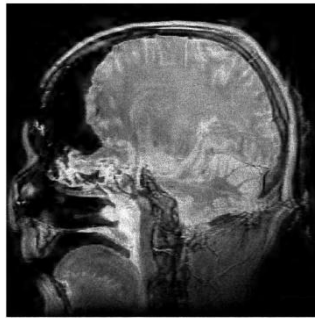


Figure 4.15 Smooth Shrink

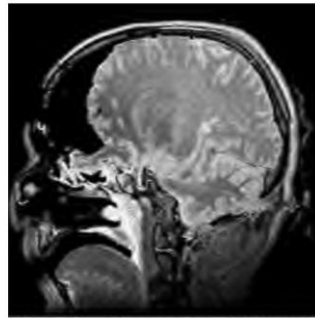


Figure 4.16 denoised using fuzzy based

Performance of wavelet filters on Ultrasound baby image ,which contaminated by speckle noise of standard deviation of 45

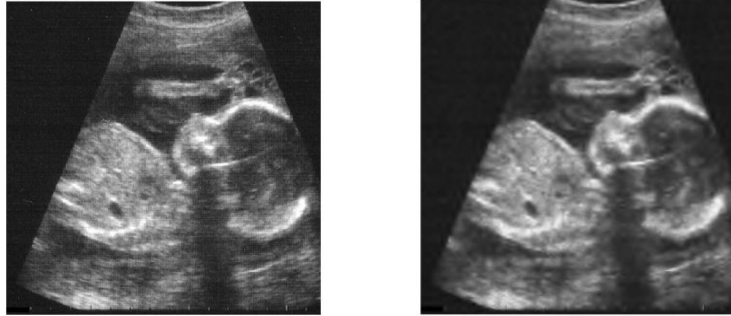


Figure 4.21 denoised image using sureshrink

Figure 4.17 original ultrasound image



Figure 4.18 speckle noise of standard deviation 45



Figure 4.19 denoised using bayes shrink



Figure 4.22 denoised image using visushrink



Figure 4.23 denoised using neigh shrink



Figure 4.24 denoised using oracle shrink



Figure 4.25 denoised using smooth shrink



Figure 4.26 denoised image using fuzzy

# Chapter5

## **Conclusion and Future Work**

## 5.1 Conclusion

### Spatial domain filters

Noise can be removed using Linear spatial domain filters as well transform domain filters. Linear techniques possess mathematical simplicity but have the disadvantage that they introduce blurring effect. To reduce this blurring effect we can use non-linear filters like median filter etc. Here the considered are AWGN and Speckle Noise. Speckle Noise uses the advantage of logarithmic transform. Among the spatial domain filters Lee filter is good edge preserving filter. From chapter 3, it is cleared that Wiener and Lee filter having  $3 \times 3$  window size are giving efficient results under low noise variance. Anisotropic diffusion is also a powerful filter where local image variation is measured at every point, and pixel values are averaged from neighborhoods whose size and shape depend on local variation, it uses partial differential equations. This is iterative filter. More iteration may lead to instability where, in addition to edges noise becomes prominent. Mean and median  $3 \times 3$  filter giving good results under low noise variance conditions and for medium noise variance conditions mean and median  $5 \times 5$  window sized filters are giving efficient results.

### Wavelet domain filters

Image denoising, using wavelet techniques are effective because of its ability to capture the energy of signal in a few high transform values, when natural image is corrupted by Gaussian noise. Wavelet thresholding, an idea that noise is removed by killing coefficient relative to some threshold. Out of various thresholding techniques soft-thresholding proposed by Donoho and Johnstone is most popular. The use of universal

threshold to denoise images in wavelet domain is known as VisuShrink , In addition, subband adaptive systems have superior performance, such as SureShrink BayesShrink, NeighShrink.

From the PSNR and UQI values in the chapter 4, it is clear that Neigh Shrink filter giving better results under low noise variance conditions and fuzzy based shrinkage giving moderate results under medium and high noise variance conditions

As Speckle noise is inherent property of ultrasound images. From the above simulated values , neigh shrink yields good performance under low variances of noise. And in case of high noise variance , neigh shrink , bayes shrink and fuzzy based wavelet denoising technique give the good filtering performance.

As execution time is another important image metric it is observed that bayes shrink and neigh shrink are taking more time(in seconds) than fuzzy based wavelet filter.

## **5.2 Scope for future Work**

There is sufficient scope to develop very effective filters in the directions mentioned below.

- (a) The widow size and the shape of the window can also be varied and made adaptive to develop very effective denoising.
- (b) Some other transforms such as DHT, curvelet and slantlet can be used for image denoising.
- (c) neural network can be employed to get efficient filters.

## References

- [1] R.C. Gonzalez and R.E. Woods, *Digital Image Processing*, 2nd ed. Englewood Cliffs, NJ: Prentice-Hall; 2002.
- [2] A.K. Jain, *Fundamentals of Digital Image Processing.*, Englewood Cliffs, NJ: Prentice Hall; 1989.
- [3] S.Sudha, G.R.Suresh and R.Sukanesh, "Speckle Noise Reduction in Ultrasound Images by Wavelet Thresholding based on weighted Variance", *International Journal of Computer Theory and Engineering*, Vol. 1, No. 1, April 2009.
- [4] N.Bhoi, S. Meher, "Circular Spatial Filtering under High Noise Variance Conditions ," *Computers & Graphics*, Elsevier ,vol. 32, issue 5, October 2008, pp. 568-580.
- [5] M Mastriani and A.E. Giraldez, "Smoothing of coefficients in wavelet domain for speckle reduction in synthetic aperture radar images", *Journal of Graphics Vision and Image Processing*, vol. 7(special issue), pp. 1-8, 2007.
- [6] X. Wang, "Lee filter for multiscale image denoising," *Proceedings of international conference on signal processing*, vol. 1, 2006.
- [7] Oleg V. Michailovich and Allen Tannenbaum, " Despeckling of Medical Ultrasound Images" , *IEEE transactions on ultrasonics, ferroelectrics, and frequency control*, vol. 53, no. 1, january 2006
- [8] M. Kazubek, "Wavelet domain image denoising by thresholding and Wiener filtering," *IEEE Signal Processing Letters*, vol.10, no. 11, pp. 324-326, 2003.
- [9] D.L. Donoho, I.M. Johnstone, "De-noising by soft-thresholding," *IEEE Transactions on Information Theory*, vol. 41, no. 3, pp. 613–27, 1995.
- [10] N.Bhoi, S. Meher, "Gaussian noise removal using anisotropic diffusion," Proc. In National Conference on Nascent Technologies in the Engineering, NCNTE-2008.
- [11] S. Meher, Development of Some Novel Nonlinear and Adaptive Digital Image Filters for Efficient Noise Suppression, Doctoral Dissertation, National Institute of Technology, Rourkela, India.
- [12] Nilamani Bhoi, Development of Some Novel Spatial-Domain and Transform-

- Domain Digital Image Filters , Doctoral Dissertation, National Institute of Technology, Rourkela, India.
- [13] S. Chang, B. Yu, M. Vetterli, “Adaptive wavelet thresholding for image denoising and compression”, *IEEE Transactions on Image Processing*, vol. 9, no. 9, pp. 1532-1546, 2000.
- [14] C. Tomasi, R. Manduchi, “Bilateral filtering for gray and color images,” *Proceedings of IEEE international conference on computer vision*, pp. 839- 846, 1998.
- [15] D.L. Donoho, I.M. Johnstone, “Adapting to unknown smoothness via wavelet shrinkage”, *Journal of the American Statistical Association*, vol. 90(432), pp. 1200-1224, 1995
- [16] Stefan Schulte and Bruno Huysmans,” A New Fuzzy-based Wavelet Shrinkage Image Denoising Technique “, *international conference on image processing*.
- [17] Sarita Dangeti, Denoising Techniques-a comparision, Doctoral Dissertation, Louisiana State University and Agricultural and Mechanical College
- [18] J.S. Lee, “Speckle suppression and analysis for synthetic aperture radar images,” *Optical Engineering*, vol. 25, no. 5, pp. 636-643, 1986.
- [19] L. A. Zadeh,”Fuzzy Logic”, *IEEE Computer Megazine*, pp. 83-93, April, 1988.